

İSTANBUL TECHNICAL UNIVERSITY ★ INSTITUTE OF SCIENCE AND TECHNOLOGY

**EFFECT OF RELATIVE VOLATILITY ON TEMPERATURE
BASED INFERENTIAL CONTROL OF TERNARY REACTIVE
DISTILLATION COLUMNS**

**M.Sc. Thesis by
Denizhan YILMAZ**

Department : Chemical Engineering

Programme : Chemical Engineering

JUNE 2010

**EFFECT OF RELATIVE VOLATILITY ON TEMPERATURE
BASED INFERENTIAL CONTROL OF TERNARY REACTIVE
DISTILLATION COLUMNS**

**M.Sc. Thesis by
Denizhan YILMAZ
(506061008)**

**Date of submission : 07 May 2010
Date of defence examination: 14 June 2010**

**Supervisor (Chairman) : Ass.Prof. Dr. Devrim B. KAYMAK (ITU)
Members of the Examining Committee : Prof.Dr. Dursun Ali ŞAŞMAZ (ITU)
Prof.Dr. Ersan KALAFATOĞLU (MU)**

JUNE 2010

İSTANBUL TEKNİK ÜNİVERSİTESİ ★ FEN BİLİMLERİ ENSTİTÜSÜ

**RELATİF UÇUCULUĞUN ÜÇ BİLEŞENLİ REAKTİF
DİSTİLASYON KOLONLARININ SICAKLIĞA DAYALI DOLAYLI
KONTROLÜNE ETKİSİ**

**YÜKSEK LİSANS TEZİ
Denizhan YILMAZ
(506061008)**

Tezin Enstitüye Verildiği Tarih : 07 Mayıs 2010

Tezin Savunulduğu Tarih : 14 Haziran 2010

**Tez Danışmanı : Yrd. Doç. Dr. Devrim B. KAYMAK (İTÜ)
Diğer Jüri Üyeleri : Prof.Dr. Dursun Ali ŞAŞMAZ (İTÜ)
Prof.Dr. Ersan KALAFATOĞLU (MÜ)**

HAZİRAN 2010

FOREWORD

I would like send my gratitude and thanks to my supervisor, Associate Professor Doctor Devrim Baris Kaymak for his patience, guidance, review and editing of the manuscript, throughout my graduate dissertation.

I am also grateful to my wife Pınar Üner Yılmaz for her motivation and invaluable encouragement during this study.

I acknowledge the financial support from the Scientific and Technological Research Council of Turkey (TÜBİTAK) through the project with grant number 108M504.

I would like to express my thanks to all my teachers who have contributions to me; I remain theirs respectfully.

Last but not least, I offer my grateful thanks to my beloved family; for their unwavering support and love.

May 2010

Denizhan Yılmaz

Chemical Engineering

TABLE OF CONTENTS

	<u>Page</u>
ABBREVIATIONS.....	vii
LIST OF TABLES.....	ix
LIST OF FIGURES.....	xi
LIST OF SYMBOLS.....	xiii
SUMMARY.....	xv
ÖZET.....	xvii
1. INTRODUCTION.....	1
2. BACKGROUND.....	5
2.1. Reactive Distillation Design.....	5
2.2. Reactive Distillation Control.....	8
3. DESIGN AND CONTROL FUNDAMENTALS.....	15
3.1. Process Studied.....	15
3.2. Assumptions and Specifications.....	18
3.3. Steady State Design and Procedure.....	19
3.4. Sizing and Economics.....	23
3.5. Process Control.....	24
3.5.1. Control Structure CS1.....	25
3.5.2. Control Structure CS2.....	26
3.5.3. Control Structure CS3.....	27
3.5.4. Selection of Temperature Control Trays.....	28
3.5.6. Controller Tuning.....	28
4. RESULTS AND DISCUSSION.....	31
4.1. Effect of Design Variables.....	31
4.2. Effect of Relative Volatility.....	32
4.3. Controllability of Base Case Design for Different Relative Volatility Cases.....	35
4.3.1. Control Structure CS1.....	35
4.3.2. Control Structure CS2.....	38
4.3.3. Control Structure CS3.....	41
4.4. Controllability of Optimum Designs for Different Relative Volatility Cases.....	45
4.4.1. Control Structure CS1.....	45
4.4.2. Control Structure CS2.....	47
4.4.3. Control Structure CS3.....	50
5. CONCLUSIONS.....	55
REFERENCES.....	57
CURRICULUM VITAE.....	61

ABBREVIATIONS

ATV	: Auto-tuning method
BuAc	: Butyl acetate
CC	: Capital Cost
CE	: Energy Cost
EQ	: Equilibrium state model
EtAc	: Ethyl acetate
ETBE	: Ethyl <i>tert</i> -butyl ether
MeAc	: Methyl acetate
MTBE	: Methyl <i>tert</i> -butyl ether
NEQ	: Non-equilibrium state model
P	: Proportional
PI	: Proportional-integral
RD	: Reactive Distillation
SVD	: Singular value decomposition
TAC	: Total Annual Cost
TAME	: <i>Tert</i> -amyl methyl ether

LIST OF TABLES

Page

Table 3.1 : Kinetic and Physical Parameters	15
Table 3.2 : Vapor Pressure Constant.....	18
Table 4.1 : Results of the Base Case	33
Table 4.2 : Results of the Optimum Design	34
Table 4.3 : Tuning Parameters of CS1.....	36
Table 4.4 : Tuning Parameters of CS2.....	39
Table 4.5 : Tuning Parameters of CS3.....	42
Table 4.6 : Tuning Parameters of CS1.....	46
Table 4.7 : Tuning Parameters of CS2.....	48
Table 4.7 : Tuning Parameters of CS3.....	50

LIST OF FIGURES

Page

Figure 3.1	: Ternary Reactive Distillation Column	14
Figure 3.2	: Vapor pressures for the temperature-dependent relative volatilities...	17
Figure 3.3	: Equilibrium-Based Stage Model.....	19
Figure 3.4	: A Feedback Control Loop	25
Figure 3.5	: Control Structures: a) CS1 b) CS1-FR.....	26
Figure 3.6	: Control Structure CS2.....	27
Figure 3.7	: Control Structure CS3.....	27
Figure 3.8	: Block Diagram of a Relay Feedback System.....	29
Figure 3.9	: Typical Relay Feedback Response.....	29
Figure 4.1	: Effects of Design Variables.....	31
Figure 4.2	: Effect of Pressure on Temperature Profile.	32
Figure 4.3	: Effect of Relative Volatility on Temperature Profile.....	33
Figure 4.4	: Temperatures of Profiles of Optimum Designs for Three Different Cases.....	34
Figure 4.5	: Compositions of Profiles of Optimum Designs for Three Different Cases.....	35
Figure 4.6	: Steady-state Gains and SVD Analysis.....	36
Figure 4.7	: Results of a) CS1 b) CS1-FR for +20% F_{0B} Step Change	37
Figure 4.8	: Steady State Variation in Controlled Reactive Tray Temperature.....	38
Figure 4.9	: Steady-state Gains and SVD Analysis.....	39
Figure 4.10	: Results of control structure CS2: a) +20% F_{0A} , b) -20% F_{0A}	40
Figure 4.11	: The Transient Stoichiometric Imbalance ($F_{0B} - F_{0A}$) for the Base Case.....	41
Figure 4.12	: Steady-State Gains and SVD Analysis.....	42
Figure 4.13	: Result of Control Structure CS3: a) +20% VS b) -20% VS	43
Figure 4.14	: Result of Control Structure CS3: a) $z_{0A(B)} = 0.05$, and b) $z_{0A(C)} = 0.05$	45
Figure 4.15	: Steady-State Gains and SVD Analysis.....	46
Figure 4.16	: Result of Control Structure CS1: +20% F_{0B} Step Change.....	47
Figure 4.17	: Steady-State Gains and SVD Analysis.....	48
Figure 4.18	: Result of Control Structure CS2: a) +20% F_{0A} b) -20% F_{0A}	49
Figure 4.19	: Steady-State Gains and SVD Analysis.....	50
Figure 4.20	: Result of Control Structure CS3: a) +20% VS b) -20% VS	52
Figure 4.21	: Result of Control Structure CS3: a) $z_{0A(B)} = 0.05$, and b) $z_{0A(C)} = 0.05$	45

LIST OF SYMBOLS

A	reactant component
a	amplitude of output response
a_F	preexponential factor for the forward reaction ($\text{kmol.s}^{-1}.\text{kmol}^{-1}$)
a_R	preexponential factor for the reverse reaction ($\text{kmol.s}^{-1}.\text{kmol}^{-1}$)
A_C	heat exchanger area for condenser (m^2)
A_R	heat exchanger area for reboiler (m^2)
A_{VP}	vapor-pressure constant
B	reactant component
B	bottoms flow rate in the column (mol.s^{-1})
B_{VP}	vapor-pressure constant
C	product component
D_C	diameter of the column (m)
E_F	activation energy of the forward reaction (cal.mol^{-1})
E_R	activation energy of the reverse reaction (cal.mol^{-1})
F_{0i}	fresh feed flow rate of reactant i (mol.s^{-1})
f	detuning factor
h	relay magnitude
k_F	specific reaction rate of the forward reaction ($\text{kmol.s}^{-1}.\text{kmol}^{-1}$)
k_R	specific reaction rate of the reverse reaction ($\text{kmol.s}^{-1}.\text{kmol}^{-1}$)
K_C	controller gain
K_{EQ}	equilibrium constant
K_P	steady-state gain
K_U	ultimate gain
L_C	length of the column (m)
L_i	liquid flow rate from tray i (mol/s)
L_R	liquid flow rate in the rectifying section (mol/s)
M_B	liquid holdup in the column base (mol)
M_D	liquid holdup in the reflux drum (mol)
M_i	liquid holdup on tray i (mol)
M_w	molecular weight of all species in the mixture (g/mol)
M_j	liquid holdup on tray j (mol)
M_{RX}	liquid holdup on each tray in the reactive section (mol)
N_C	number of component
N_R	number of rectifying trays
N_{RX}	number of reactive trays
N_S	number of stripping trays
N_T	number of trays in the column
P	column pressure (bar)
P_U	ultimate period (min)
$P_{j,i}^S$	vapor pressure of component i on tray j (bar)
R	reflux flow rate (mol/s)
$r_{j,i}$	reaction rate of component i on tray j (mol/s)

T_j	column temperature on tray j (K)
V_i	vapor flow rate on tray j (mol/s)
V_{NT}	molar flow rate from the top of the column (mol/s)
V_S	vapor boilup (mol/s)
U_C	overall heat-transfer coefficient in the condenser ($\text{kJ.s}^{-1}.\text{K}^{-1}.\text{m}^{-2}$)
U_R	overall heat-transfer coefficient in the reboiler ($\text{kJ.s}^{-1}.\text{K}^{-1}.\text{m}^{-2}$)
U	left singular vector matrix
V	right singular vector matrix
$x_{B,i}$	bottoms composition of component i in liquid
$x_{j,i}$	liquid mole fraction of component i on tray j
$y_{j,i}$	liquid mole fraction of component i on tray j
z_{0i}	fresh feed mole fraction of component i

Greek Symbols

α	relative volatility
α_{ji}	relative volatility of component j to component i
α_{390}	relative volatility at 390 K
β_{pay}	payback period (year)
ΔH_V	heat of vaporization, cal/mol
λ	heat of reaction, cal/mol
ν_i	stoichiometric coefficient of component i
Σ	diagonal matrix of singular values
τ_i	reset time (min)

EFFECT OF RELATIVE VOLATILITY ON TEMPERATURE BASED INFERENTIAL CONTROL OF TERNARY REACTIVE DISTILLATION COLUMNS

SUMMARY

The growing environmental and economic concerns, bring up the interest in the reactive distillation columns that unites reaction and separation processes in one unit. The most common area of usage of these columns is two reactants – two products and two reactants – one product exothermic reactions systems. However, the effect of relative volatility on steady state design and inferential control for ternary two reactants – one product exothermic reactions systems has not been examined in literature.

In order to bridge the gap in this field, in the first part of the study, the effect of relative volatility of components to steady state designs has been examined. First of all, a steady state column design was built for the chemicals which assumed having relative volatilities between the components constant at 2. The RD column has been optimized using three optimization variables such as the number of stripping section, number of reactive section and operating pressure. This design has the minimum Total Annual Cost (TAC) and it was taken as a base case for the rest of the study. Afterwards, the impact of the feed of the chemicals having different relative volatilities, for the base case was examined. It has been found that the system needs more vapor boilup as the relative volatilities get closer, which results in an increase of the energy cost. Next, optimum steady state designs have been obtained for the chemicals having temperature-dependent relative volatilities. In this case, besides the increasing values of vapor boilups, column diameter and the heat transfer areas of reboiler and condenser, RD column requires more separation trays as relative volatilities get closer. In the second part of the study, temperature based inferential control structure with three different control scheme was designed for the steady state columns. Firstly, Singular Value Decomposition (SVD) method and sensitivity analysis were used to choose the most sensitive tray in column for the change of manipulated variable in designed control structures. As a result of these analyses, the trays were found for each steady state design. After that, temperature loops were manipulated which will be controlling the sensitive trays, by the Relay Feedback Test (ATV) method. The performance of temperature based inferential control structures has been examined in the face of different disturbances. It is observed that only one control structure (CS3) effectively controls the systems for different relative volatility cases. On the other hand, no significant effect of the relative volatilities has been observed on the temperature based inferential control of the ternary RD columns.

RELATİF UÇUCULUĞUN ÜÇ BİLEŞENLİ REAKTİF DİSTİLASYON KOLONLARININ SICAKLIĞA DAYALI DOLAYLI KONTROLÜNE ETKİSİ

ÖZET

Giderek önem kazanan çevresel ve ekonomik kaygılar, reaksiyon ve ayırma işlemlerini tek üniteye birleştiren reaktif distilasyon kolonlarının kullanımına olan ilgiyi de beraberinde getirmektedir. Bu kolonların en yaygın kullanım alanı, iki reaktan-iki ürün ve iki reaktan-bir ürün içeren ekzotermik reaksiyon sistemleridir. Fakat literatürde iki reaktan-bir ürün içeren reaksiyon sistemleri için bileşenler arasındaki bağıl uçuculuğun yatışkın hal tasarım ve kontrolüne etkileri incelenmemiştir.

Alandaki bu boşluğu kapatmak adına, çalışmanın ilk aşamasında, bileşenlerin bağıl uçuculuklarının değişimlerinin yatışkın hal tasarımlarına etkileri incelenmiştir. İlk olarak, birbirleri arasındaki bağıl uçuculukların sıcaklıktan bağımsız sabit iki olduğu kabul edilen kimyasallar için yatışkın hal kolonu tasarımı yapılmıştır. Bu kolon, optimizasyon değişkenleri olan sıyırma rafı sayısı, reaktif raf sayısı ve operasyon basıncı kullanılarak optimize edilmiştir. Optimizasyonu yapılan kolon, toplam yıllık maliyet açısından minimum değere sahiptir ve çalışmanın daha sonraki aşamalarında temel tasarım olarak ele alınmıştır. Daha sonra, mevcut olan temel tasarıma farklı bağıl uçuculuğa sahip kimyasalların beslenmesi sonucu oluşacak etkiler incelenmiştir. Bağıl uçuculuğun etkilerin incelenmesinde kimyasalların bağıl uçuculuklarının sıcaklığa bağlı ve sıcaklık artışıyla uçuculukları birbirine yaklaşan kimyasallar olduğu düşünülmüştür. Elde edilen tasarım sonuçları, bağıl uçuculuklar birbirine yaklaşırken kolon için gerekli olan enerji maliyetlerinin arttığını göstermiştir. Sonraki aşamada, bağıl uçuculukları sıcaklığa bağlı, sıcaklık artışıyla uçuculukları birbirine yaklaşan bu kimyasallar için optimum yatışkın hal kolon tasarımları elde edilmiştir. Kimyasalların relatif uçuculuklarının azalması sonucu ihtiyaç duyulan buhar debisinin artmasının yanı sıra kolon çapı, reboyer ve kondenser ısı transfer alanları artmıştır.

Çalışmanın ikinci kısmında ise yatışkın hal tasarımları yapılan kolonlar için üç farklı sıcaklığa dayalı dolaylı kontrol yapısı tasarlanmıştır. İlk olarak, tasarlanan kontrol yapılarındaki ayarlanan değişkenlerin kolon içerisindeki değişimlerine en hassas rafı seçmek amacıyla hassaslık analizi ve tekil değer ayrışması (SVD) yöntemi kullanılmıştır. Yapılan analizler sonucu her bir yatışkın hal tasarımı için kontrol edilecek raflar bulunmuştur. Daha sonra hassas raflardaki sıcaklığı kontrol edecek sıcaklık kontrol çevrimleri, otomatik ayar yöntemi (ATV) kullanılarak ayarlanmıştır. Prosesler farklı bozan etkenlere maruz bırakılarak, tasarlanan sıcaklığa dayalı dolaylı kontrol yapıların etkinlikleri incelenmiştir. Tasarlanan son kontrol yapısının her üç farklı bağıl uçuculuk durumu için de değişik bozan etkenlere karşı etkili olduğu görülmüştür. Diğer yandan, kimyasalların bağıl uçuculuklarının, üçlü RD kolonlarının sıcaklığa bağlı dolaylı kontrolü üzerine etsinin olmadığı görülmüştür.

1. INTRODUCTION

Around the world, a significant fraction of capital investment and operating cost involves separation almost in all of the chemical industries. Distillation is the most common separation technique based on differences in their volatilities in a boiling liquid mixture and is energy intensive. Distillation can consume more than 50% of a plant's operating energy cost.

Chemical reactors are also essential parts of many chemical processes because they transform raw materials into valuable chemicals. Reactor effluents contain mostly products but also unconverted reactants or by-products. Therefore, many chemical processes involve separation unit to obtain high purity product. On the other hand, due to increased energy demand and environmental concerns worldwide, important research is currently underway on process intensification. Process intensification gains more and more in importance and interest in many fields, leading to the development of novel equipment and techniques which advance the chemical processes with respect to decreased costs with reduced equipment size, increased energy efficiency, less waste and pollution, improved safety. Reactive distillation (RD) is considered as a key technology because of its high potential for process intensification. RD combines both separation and reaction in a single column in which chemical reaction and product separation occur simultaneously. The combination can lead to both economic and environmental gains resulting from the process intensification.

A reactive distillation column usually consists of three sections: reactive section, stripping section and rectifying section. In the reactive section, the reactants are transformed into products and then by the distillation process the products are separated out of reactive zone. The errands of rectifying and stripping sections are highly reliant on the boiling points of the reactant and product. The rule of building a RD column is simple. A reactive distillation column is a distillation column having a catalyst zone strategically placed in the column to carry out the desired reaction. The catalyst can be either in the same phase with the reacting species or in the solid

phase. The feed for the process is fed either above or below the reactive zone depending upon the volatility of the components and to carry out the desired reaction. The reaction occurs mainly in the liquid phase, in the catalyst zone [1,2].

RD columns provide numerous advantages over conventional reactor/ separation configurations. The main advantages of RD column include: (1) reducing capital investment and operational costs (recycle, pumps, piping etc.) by combining two equipments into one unit, (2) overcoming chemical equilibrium limitation through continuously removing the products from column, (3) eliminating the limitation of azeotropic mixture separation by the presence of reaction (reacting away), (4) increasing energy efficiency by the internal heat integration of heat of reaction and separation, (5) increasing reaction selectivity since elimination of possible side reactions by removal of the products from the reaction zone [1,2].

Reactants and products are continuously separated from the liquid reaction phase into the nonreactive vapor phase in RD column. This characteristic allows an enhanced conversion and reaction rate in equilibrium limited reversible reactions, a higher product selectivity in the case of multiple competing reactions, and provides an efficient means of heat removal from the liquid phase for reactions with high heat of reaction. However, because heat transfer, mass transfer, and reactions are all occurring simultaneously, the dynamics that can be exhibited RD columns can be more complex than found in regular columns. During reactive separations, complex interactions between vapor-liquid mass and energy transfer and chemical kinetics occur strong nonlinearities. This results increase the complexity of process operations and the control structure installed to regulate the process.

The suitability of RD for a particular reaction depends on various factors such as relative volatilities between reactants and products, distillation and reaction temperature. The volatilities between reactants and products must be suitable to ensure high concentrations of reactants and low concentrations of products in reactive section. Another important limitation is the temperature suitability for reaction and separation since both operations occur in the same unit at the same pressure. Low temperatures decrease specific reaction rates thus, very large holdups (or large amounts of catalyst) and more separation trays will be needed. High temperatures decrease chemical equilibrium constants for exothermic reversible reactions and these may also cause undesirable side reactions. If the chemical

equilibrium constant decreases, the reaction will reverse so that the conversion cannot be the desired product conversion. In either low or high temperatures in RD can provoke hydraulic limitations as well. So, the use of RD for every reaction may not be feasible and economical. RD is especially suited for equilibrium-limited liquid-phase reactions where the products and reactants have suitable volatility. The investigation of the candidate reactions for RD is an area that needs considerable attention to enhance the domain of RD processes [1-3].

All the factors that are stated above contribute to the growing academic and commercial importance of RD columns. Research on various aspects such as modeling and simulation, column hardware design, non-linear dynamics and control is in progress.

RD columns has been studied both real chemical systems and ideal hypothetical systems in literature and textbooks [1,2]. Ideal hypothetical reaction systems have been usually used to discuss the importance of key design parameters such as pressure, reactive zone location, number of reactive trays, holdup on a reactive tray, etc. In addition, it is used to synthesize control scheme for RD columns. The results obtained from ideal systems are used for generalization of other reaction systems which are similar in terms of design, stoichiometry, reaction kinetics and vapor-liquid equilibrium. Therefore, to examine the effect of relative volatility, a hypothetical generic system has been studied.

Although two reactant-two product generic systems have been widely studied, there are relatively few papers dealing with two reactant-one product systems[1]. Moreover, for two reactant-one product systems, there is no research on the effect of the relative volatility differences among the components. The relative volatility differences could affect ternary RD column design and control. Therefore, in this study, how the relative volatility differences among the components affect the RD column configurations and the design and robustness of temperature based inferential control structures have been investigated. For all these structures, conventional linear state feedback controllers have been used. Thus, it is difficult to design nonlinear controller that requires extra information about the system. The nonlinearity between controlled variable (output) and manipulated variable (input) can limit the usage of conventional linear controller. That is why the use of linear controller is another point in the study.

The aim of this study is to investigate how the relative volatility differences among the components affect the temperature profiles of different RD column configurations, and relatedly the design and robustness of temperature based inferential control structures.

This dissertation will provide a datasheet of investigating the design parameters in terms of TAC and profound information on how the controllability of RD columns of ternary systems using control structures including temperature based inferential control are affected by the relative volatility differences among the components. With the help of the information gained from the research, for ternary RD column configurations with different chemical systems, effective control structures including inferential temperature measurements can be proposed.

2. BACKGROUND

Although reactive distillation was invented in 1921 [4], the industrial application of RD did not take place before the 1980s. The patents and literature on RD columns have increased rapidly in the last two decades. According to a recent book on RD design and control, there are 236 different reaction systems which have been studied [1]. The most studied reaction types are the quaternary systems ($A+B\leftrightarrow C+D$) with 91 examples and the ternary systems ($A+B\leftrightarrow C$) with 60 examples. RD columns have been successfully implemented for esterification and etherification systems in the industry. The production of ethyl acetate (EtAc), butyl acetate (BuAc) and methyl acetate (MeAc) are important esterification applications, while the production of methyl *tert*-butyl ether (MTBE), ethyl *tert*-butyl ether (ETBE), and *tert*-amyl methyl ether (TAME) are important etherification applications for RD systems.

2.1. Reactive Distillation Design

The design and operation issues of RD columns are more complicated than either conventional reactors or conventional distillation columns. Separation and reaction occurring simultaneously in a single unit results in complex interactions of vapor-liquid equilibrium, vapor-liquid mass transfer and chemical kinetics. To understand the dynamic behavior of RD columns, these interactions should be depicted by having a model of the process. In literature, the most common models that have been reported are the equilibrium state model (EQ) consisting of MESH (material balance, vapor-liquid equilibrium equations, mole fraction summations, and heat balance) equations and the non-equilibrium state model (NEQ) consisting of the so-called MERQ (material balance, energy balance, rate equations for mass transfer, and phase equilibrium at vapor-liquid interface) equations which are also known as the rate-base models. The equilibrium based model is assumed that the bulk vapor and the bulk liquid phase are in thermodynamic equilibrium with each other. Thus, there is no temperature gradient within the state where the equilibrium assumption is valid.

In a non-equilibrium model, the liquid and vapor interface is assumed to be in equilibrium. Mass transfer takes place at the interface of the bulk phases, and also inside these phases. Therefore, a temperature gradient occurs through the phases [3].

The application and development of the EQ stage model for conventional distillation columns have been reported in several textbooks and review articles [3,5,6]. These models have been adopted to RD columns by adding reaction terms. The EQ stage model have been modified for RD by adding the rate of the reaction term to the material balance equations and by the inclusion of heat of reaction term into the energy balance equations [7-10].

The NEQ stage model for RD follows the same approach and methodology of the rate-based models used for conventional distillation [11-12]. Lee and Dudukovic reported the comparison of the equilibrium model with the non-equilibrium model for an esterification reaction between ethanol and acetic acid. They proposed that the NEQ stage model is to be preferred for the simulation of RD compared to an equilibrium based model because of the difficulty associated with the prediction of tray efficiencies [13]. Krishna and co-workers also studied the comparison of the equilibrium model with the non-equilibrium model for RD columns. It has been shown that the NEQ modelling approach affects the hardware design, which might have a significant influence on the conversion and selectivity [14].

On the other hand, the complexity of the modeling increases greatly if mass transfer and/or reaction kinetics are taken into account. The NEQ stage model is more complex and requires thermodynamic properties, not only for phase equilibrium, but also for the calculation of the driving forces of mass transfer accompanied by chemical reactions. In addition, the mass and heat transfer coefficients, interfacial areas and physical properties such as surface tension, diffusion coefficients, viscosities, etc are required. Therefore, the NEQ stage models have been usually used for commercial RD column designs [3,11,12].

Since the EQ stage models have less empirical parameters, the usage of this approach is more convenient for the design of ideal systems and control purposes. Thus, the EQ stage models have been used for several studies on RD.

Using the EQ stage model, Kaymak and Luyben compared the design of a RD column with a conventional multi-unit reactor/column/recycle process for a

quaternary reaction system. The reaction considered is a generic exothermic reversible reaction system including two reactants and two products. Each flowsheet has been optimized in terms of the total annual cost (TAC) for a wide range of chemical equilibrium constants K_{EQ} . They showed that the RD configuration has lower capital and energy costs than the conventional configuration for all kinetic cases [15]. They also demonstrated that TAC increases as the value of chemical equilibrium constant decreases for quaternary systems [16].

Luyben and co-workers also studied the design and control of two alternative processes for the production of butyl acetate. One of them is a conventional reactor/separator process, while the other one includes a RD column. They showed that the TAC of the process including a RD unit is 20% lower than that of the conventional process [17].

Kaymak and Luyben further represented the quantitative comparison of RD and conventional reactor/separator systems for a quaternary system. They investigated effects of relative volatility on the design of the flowsheets. Two type of changes in relative volatility were considered. Firstly, relative volatilities between adjacent products and reactants were independent of the temperature, so they were kept constant through the RD but were varied for each case from 2 to 1.25. Secondly, relative volatilities of all component were temperature dependent, so they were decreased with increasing temperature. It is showed that for the constant relative volatility case, the optimum RD configuration is more economical than multi-unit system for all values of relative volatilities. For temperature-dependent case, Although the TAC of the conventional multi-unit process slightly increases as the relative volatilities decrease, both capital and energy costs of the RD column increase rapidly [18].

Yu and Tung investigated the effects of relative volatility ranking to the design of an ideal chemical reaction system. Since the reaction considered is a two-reactant and two-product system, there are 24 possible relative volatility arrangements. They optimized all arrangements in terms of the total annual cost (TAC), and demonstrated that the relative volatility rankings play a key role in RD column configurations [19].

Luyben has studied the effects of kinetic and design parameters for an ideal ternary system with a chemistry of $A+B\leftrightarrow C$. Two different cases have been considered. In the first case, there are only three components taking part in the reaction. On the

other hand, there is a fourth component fed to the process in the second case. Although this component is inert in terms of the reaction, it may affect the vapor-liquid phase equilibrium and the structure of the column. For both processes, effects of the design parameters such as number of separation trays, number of reactive trays, column pressure, and holdup on reactive trays have been examined. It has been pointed out that the presence of the inert component has a major impact on both the structure of the column and the vapor-liquid phase equilibrium [20].

The coupling of reaction kinetics and vapor-liquid equilibrium causes high nonlinear dynamic behavior. As indicated on the papers investigating the open-loop dynamics of RD columns, this high non-linearity results in the existence of steady-state multiplicities [21-24]. Recently, Kaistha and co-workers have analyzed MTBE and methyl acetate RD columns for the possibility of the steady state multiplicities. They have demonstrated that the coupling of reaction and separation causes complex input-output relationships leading to both input and output multiplicities. They have also highlighted the importance of the column specifications (operating policy) on steady state multiplicities [25].

2.2. Reactive Distillation Control

The increasing demands for energy saving and product quality require effective control systems. However, control of RD columns is a difficult task because of their complex dynamics resulting from the interaction between reaction and separation [25].

The direct way to achieve the desired conversion and product purity is using a composition analyzer that measures an internal composition in the column. However, the maintenance of composition analyzers are expensive, and they introduce large dead-times into the control loop. Therefore, reliable composition measurements may not be obtained for the control of RD columns. Thus, Roat and co-workers proposed a temperature-based inferential control structure for RD column systems to avoid the use of analyzers. This control structure was using two conventional proportional-integral (PI) temperature controllers to control two tray temperatures in the two-product RD column by manipulating two fresh feed streams. The reboiler heat input

was fixed. However, this structure could handle only a 5% increase in the throughput [26].

Later, Bock and co-workers studied esterification of myristic acid in a RD column coupled with a recovery system. A structure controlling the purities of the products was proposed for the coupled two-column reactive distillation process. The proposed control structure was simply rationing the fresh isopropanol feed to the fresh acid feed to balance the reaction stoichiometry. However, this ratio control could not effectively handle disturbances for the feed compositions [27].

Kumar and Daoutidis studied the controllability of an ethylene glycol reactive distillation column where ethylene oxide and water are the reactants. Water was fed on the top of the column, while ethylene oxide was fed on the fourth tray. In this process, ethylene glycol leaves the column from the bottoms and there is no distillate stream. The column pressure and the product composition were controlled by manipulating the condenser duty and the reboiler duty, respectively. Two fresh feeds were flow controlled. The authors claimed that the studied control structure with conventional linear PI controllers causes stoichiometry balance problem. Thus, a nonlinear controller that performs well with stability in the high-purity region was suggested [28].

Sneesby and co-workers proposed a two-point control structure for an ethyl *tert*-butyl ether (ETBE) RD column in which both product purity and conversion are controlled. They used conventional PI controllers to control a tray temperature in the stripping section by manipulating the reboiler duty and to control the conversion by manipulating the reflux flowrate. It was shown that the two-point control scheme has superior disturbance rejection capability compared to the one-point composition control scheme [29].

Al-Arfaj and Luyben explored a variety of control structures for an ideal two-reactant and two-product RD column. In their study, six alternative control structures, all of which including the composition measurement of a reactant inside the reactive section of the column was explored. This composition was controlled by adjusting the appropriate fresh feed stream. Al-Arfaj and Luyben claimed that the inventory of one of the reactants needs to be detected so that a feedback trim can balance feed stoichiometry of the reactants, unless an excess of one of the reactants

in the column is incorporated during the design stage. Thus, the use of a composition analyzer in the reactive zone was advocated [30].

Estrada-Villagrana and co-workers studied the controllability of an MTBE RD column with linear control tools. Three control schemes were analyzed to determine the best control scheme. The control schemes were constructed to control reflux drum level, the base level and MTBE purity in the bottoms. To control the drum level, the distillate and the reflux streams were considered as possible manipulating variables. The bottoms flowrate was adjusted to control the base level for each scheme. A temperature in the stripping zone was controlled by manipulating the reboiler duty to maintain the desired MTBE purity at the bottoms. Although the RD columns have highly nonlinear behaviors, they demonstrated the use of input-output control schemes with linearized control tools for the control of the RD column [31].

Vora and co-workers studied the controllability of an ethyl acetate RD column. They analyzed the system from steady-state and dynamic point of views. It was found that the process has two time scales caused by the liquid hydraulics. Control structure manipulating the reflux flow to control the acetate purity at the top of the column and the condenser duty to control the operating pressure was used. Nonlinear controllers were designed based on the two-time scale model. These nonlinear controllers performed well for a 25% increase in the product purity setpoint. However, it was demonstrated that the linear controllers for the same configuration were able to handle only a 1% product purity change [32].

Al-Arfaj and Luyben compared an ideal RD column with a methyl acetate RD column in terms of controllability. Three control structures were examined for both columns. Three compositions analyzers were used for the first control structure in which the vapor boilup and reflux flowrate were manipulated to control the purities of the bottoms and distillate streams, respectively. One of the fresh feeds was manipulated to control a composition in the reactive section of the column. One composition controller and one temperature controller was used. In the second control structure, a tray temperature was controlled in the stripping section to maintain the bottoms purity. In the third one, two temperatures were controlled by manipulating the two fresh feeds. It was demonstrated that the second control structure provides effective control of both processes. Controllability using the first structure was found difficult for the high-conversion methyl acetate column because

of the system nonlinearities. In addition, it was observed that the two-temperature control structure provides an effective control when the process is oversized [33].

This study was extended for an ETBE RD column where two different process configurations have been used. The first configuration consists of two fresh reactant feed streams, while the second configuration includes a single reactant feed. According to the results, an internal composition control of one of the reactants is required to balance the stoichiometry perfectly [34].

Despite Kumar and Daoutidis's claim [28], Al-Arfaj and Luyben demonstrated that ethylene glycol RD column can be effectively controlled by a simple PI control configuration where inferential temperature control was preferred instead of direct composition control. Their proposed control structure achieved balancing the stoichiometry of the reactants, and maintained the product purity within reasonable bounds. Since there is a big temperature change through the stripping section, the tray for temperature control was selected from this section. This tray temperature was controlled by manipulating reboiler duty. The control structure has only conventional PI loops and can handle large disturbances. It was reported that this control structure can be applicable to different systems which are similar to ethylene glycol system in terms of design, stoichiometry, reaction kinetics and vapor-liquid equilibrium [35].

Wang and co-workers investigated the effect of multiplicity on the control system design for an MTBE RD column. A tray temperature in the stripping section was controlled by manipulating the vapor boilup, while stoichiometric balance was controlled by a feed ratio plus internal composition control loop. It was demonstrated that although both input and output state multiplicities occur in the column, a linear control is still possible if controlled and manipulated variable pairings that exhibit no multiplicities can be found. They proposed that such a scheme can be found by operating at constant reflux ratio [36].

Luyben and Kaymak evaluated a two-temperature control structure for quaternary type of reactive distillation columns. Two different systems were studied; an ideal reaction system and a methyl acetate system. They demonstrated that the number of reactive trays is a key design variable, which affects the shape of steady-state gain curves. They claimed that the controllability of these columns can be increased by adding more reactive trays [37].

Kaymak and Luyben compared the effectiveness of two different inferential temperature control structures for both ideal quaternary and methyl acetate RD columns. In the first control structure, the tray temperatures were controlled by manipulating the fresh feed flowrates, and the vapor boilup was the production rate handle. On the other hand, one of the fresh feed streams and the vapor boilup were manipulated to control the tray temperatures for the second control structure. Other fresh feed stream was the production rate handle, and the feed streams were rationed. The ratio was set by the temperature controller. They pointed out that the stability of the system is seriously affected by the selection of the manipulated fresh feed stream in the second structure [38].

Kumar and Kaistha studied the performance of two temperature based inferential control structures for a methyl acetate RD column. They proposed the use of the difference between two suitably chosen reactive trays instead of using a single tray temperature, also referred to as ΔT . They claimed that controlling ΔT leads to improved robustness compared to controlling a single reactive tray temperature [39].

Luyben studied the controllability of two different ideal ternary systems with two reactants but only one product. In the first case, there are only three components. In the second, one of the feeds has an inert component in terms of reaction which affects the vapor-liquid equilibrium in the column. The author pointed out the impact of the inert component on both the configuration and control scheme design of the column [40].

In their recent papers, Kumar and Kaistha have examined the impact of steady-state multiplicity on the controllability of RD columns using two-temperature control structures. First, the nonlinear dynamic behavior of a generic ideal RD column has been explored. They demonstrated that a steady-state transition occurs for large production rate decreases, while wrong control action occurs for large production rate increases. In addition, they observed that the initial direction of response to the disturbance has an important role in determining the control system robustness [41].

Kumar and Kaistha further investigated the impact of steady-state multiplicities on the control of a methyl acetate RD column. They showed that output multiplicity for a fixed reflux ratio can lead to steady-state transition for a pulse decrease. Moreover, input multiplicity can lead to “wrong” control action for large disturbance moving

the column towards the multiplicity region. They also demonstrated that controlling a tray temperature with acceptable sensitivity provides more robust control instead of controlling the most sensitive tray temperature since the input multiplicity is avoided [42].

Later, Kumar and Kaistha examined two-point and three-point temperature control structures for an ideal quaternary RD column. They showed that the two-point control structures are unsuitable to maintain product purities for large throughput increases. They proposed that the reflux ratio must be adjusted to force the escaping reactants back into reactive zone. Therefore, they implemented three-point structures where reflux rate is manipulated to control a tray temperature in the rectifying section. They showed that both three-point control structures maintain the product purities effectively as the reflux ratio is indirectly adjusted through the manipulation of the reflux flowrate [43].

Kumar and Kaistha compared the controllability of two alternative designs of the ideal quaternary RD column. They also investigated two control structures that are limited only to temperature inferential control for the designs. It is studied bifurcation analysis that performed to understand steady-state transition and ‘wrong’ control action. They demonstrated that the number of reactive trays is the key design variable that affects the column controllability [44].

Recently, Kumar and Kaistha investigated the closed loop performance of a two-temperature control structure that has been originally proposed by Roat and co-workers. In this study, they modified the structure using ratio controllers. Three different configurations have been studied for a methyl acetate RD column. They showed that maintaining the fresh feeds in ratio does not lead to an improvement in the control performance and robustness [45].

3. DESIGN AND CONTROL FUNDAMENTALS

3.1. Process Studied

In this work, an ideal ternary system with two reactants and one product is studied. The considered reaction is a reversible liquid-phase exothermic reaction.



The relative volatilities are such that the heaviest component is the product C and the lightest component is the reactant A.

$$\alpha_A > \alpha_B > \alpha_C \quad (3.2)$$

The kinetic and physical properties are taken from the literature [20] and given in Table 3.1.

Table 3.1. Kinetic and Physical Parameters

<u>Parameter</u>	<u>Value</u>
Activation energy	
Forward	30 kcal/mol
Backward	40 kcal/mol
Specific reaction rate at 366 K(kmol s ⁻¹ kmol ⁻¹)	
Forward	0.008
Backward	0.0004
Chemical equilibrium constant at 366 K	20
Heat of reaction	-10 kcal/mol
Heat of vaporization	6.944 kcal/mol
Molecular weights A/B/C (g mol ⁻¹)	50/50/100

The flowsheet of the ternary reactive distillation column is shown in Figure 3.1. The column has two sections; a stripping section and a reactive section. Reaction occurs only in the reactive section having N_{RX} trays, and product C moves down through the column as the heaviest component. The task of the stripping section having N_S trays is to strip reactant B from the product C. There is no need to have a rectifying section, because there is no distillate at the top of the column. The column has a

partial reboiler and a total condenser that helps the column operating at total reflux. The fresh feed stream F_{OA} is fed from the bottom of the reactive section, while the fresh feed stream F_{OB} is fed from the top of the reactive section. The product C leaves the column from the bottoms. The trays are numbered starting from the bottom of the column.

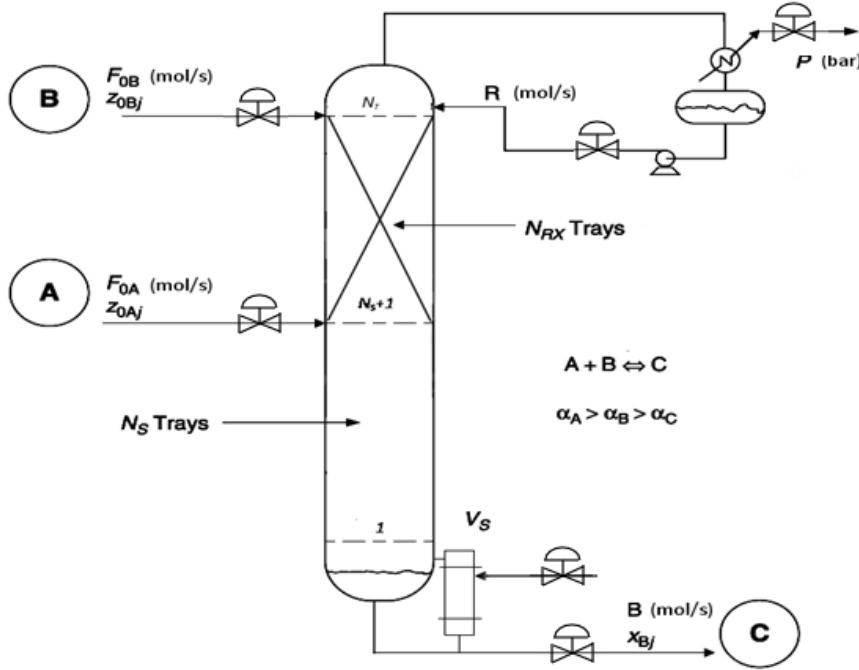


Figure 3.1: Ternary Reactive Distillation Column

Relative volatilities between adjacent components can directly affect the design variables such as the number of separating trays and the operating pressure. Relative volatility is a dimensionless quantity that compares the vapor pressures of the components in a liquid mixture of chemicals. For an ideal mixture, the relative volatility α_{ij} is equal to the ratio of the vapor pressure of component i to the vapor pressure of component j .

$$\alpha_{ij} = P_i^S / P_j^S \quad (3.3)$$

The relation between vapor pressure P^S and temperature for pure components can be described by a two-parameter Antoine equation, where A_{VP} and B_{VP} are component-specific constants.

$$\ln P_i^S = A_{VP,i} - B_{VP,i} / T \quad (3.4)$$

For the base case of this study, the relative volatilities between the components are kept constant at 2 without changing by temperature. To investigate the effect of temperature dependency of relative volatilities, the relative volatilities between adjacent components are reduced as the temperature increases. This is done by changing the relative volatilities between adjacent components at a reference temperature, while they are kept constant at 2 at a temperature of 320 K. The reference temperature is selected 390 K, and the value of α_{390} is varied over a range between 1.5 and 2. Figure 3.2 shows the vapor pressure lines for two different cases. The left graph is for the base case without any temperature dependency, while the right one is for a temperature-dependent case. The slope of the vapor pressure line of component A is same for both α_{390} cases, because the vapor pressure coefficients of this component are kept constant. However, to obtain the temperature-dependent relative volatilities, the A_{VP} and B_{VP} coefficients of other components are calculated for the specified value of the relative volatility at a temperature of 390 K. Therefore, the lines get closer while the temperature increases.

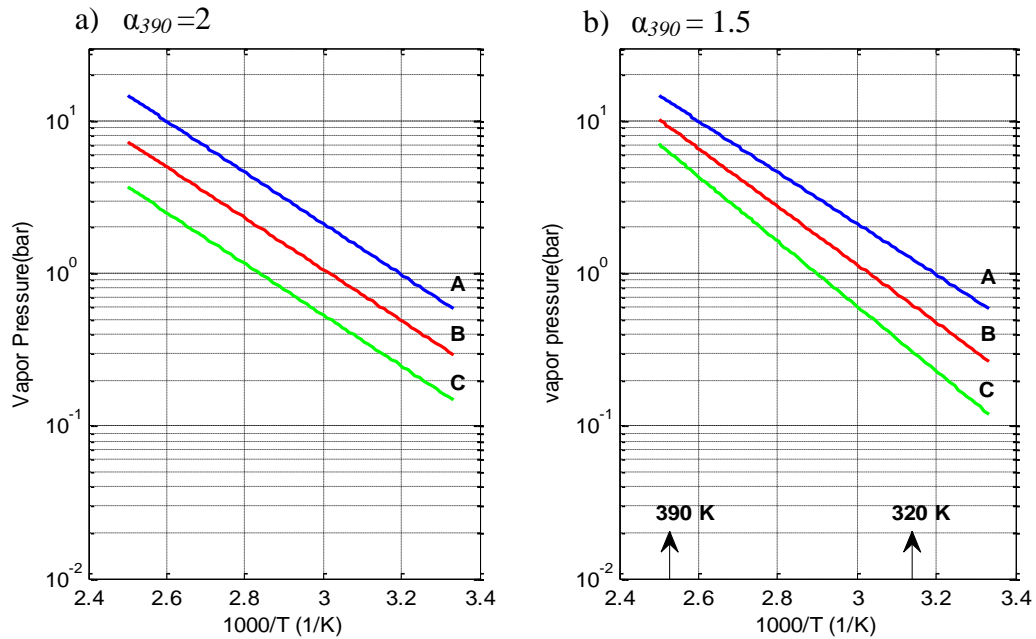


Figure 3.2: Vapor Pressures for Different Relative Volatilities: a) $\alpha_{390}=2.00$ b) $\alpha_{390}=1.5$

The vapor pressure constants of the components for three case studies are given in Table 3.2.

Table 3.2: Vapor Pressure Constants

α_{390}	Constant	A	B	C
2.00	A_{VP}	12.34	11.65	10.96
	B_{VP}	3862	3862	3862
1.75	A_{VP}	12.34	12.4	12.45
	B_{VP}	3862	4100.07	4338.13
1.50	A_{VP}	12.34	13.26	14.17
	B_{VP}	3862	4374.9	4887.8

3.2. Assumptions and Specifications

RD columns can be represented by a set of algebraic and non-linear differential equations describing the physical and chemical properties of the studied process. To find the steady state design of a RD column, the design variables of the process should be chosen carefully. In addition, there might be a large number of design variables. Therefore, following assumptions and specifications are considered in this study to reduce the number of design variables for the economically optimum steady-state design:

- (i) The kinetics holdup (M_{RX}) is assumed constant at 1000 moles
- (ii) Pressure drops in the column are neglected
- (iii) Chemical reaction occurs only in the liquid phase
- (iv) Ideal vapor-liquid equilibrium is assumed on each stage
- (v) Reflux and two fresh feed streams are saturated liquids
- (vi) Equimolal overflow is assumed in the stripping section

The design objective is to obtain a fixed production rate of product C at 12.6 mol/s with 98% purity. This means that the bottoms flow rate is $12.6/0.98 = 12.857$ mol/s. Thus, the flow rates of both fresh feed streams F_{0A} and F_{0B} require an amount of 12.6 mol/s at least. Since reactant B is heavier than reactant A, the impurity of the bottoms contains mostly reactant B. Therefore, the fresh feed flow rate of reactant B is larger than that of reactant A.

Based on these specifications and assumptions, there are three optimization variables: the number of trays in reactive zone N_{RX} , the number of trays in stripping section N_S , and the column pressure P .

3.3. Steady-State Design and Procedure

In many cases, it has been proven that the equilibrium stage model used for the simulation of distillation columns without chemical reactions can be implemented for the simulation of reactive distillation columns as well [9,10]. As shown in Figure 3.3, vapor rising from the stage below and liquid flowing down from the stage above contact each other on a stage together with any fresh feed. The vapor and liquid streams departing from the stage are assumed to be in equilibrium with each other. Using a sequence of these equilibrium stages, a complete separation process is modeled.

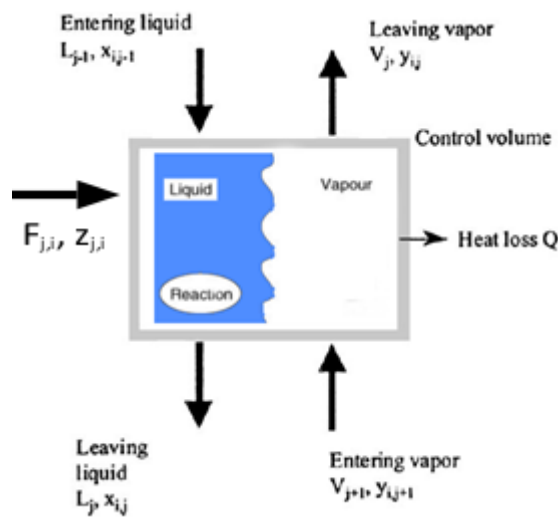


Figure 3.3: Equilibrium-Based Stage Model

A distillation column can be described by a group of equations modeling the equilibrium stages. Using the known MESH-equations (material, equilibrium, summation and heat equations), an equilibrium stage j can be described. Moreover, due to the proceeding reaction, the molar change in the number of moles of component i must be considered [10].

The simulation solution of RD is found by the simultaneous solution of material, energy balances and stoichiometric relationships, which corresponds to the solution of a considerable large set of non-linear equations. The relaxation method is a reliable and efficient technique in solving this large set of equations [46,47]. This method uses the equilibrium-stage model equations in unsteady-state material balances. Liquid mole fractions and temperatures on each stage are designated as initial guess. During repeated computations, the mole fractions are proceeded

towards the steady state values by relaxation method. Steady-state solution is found through the change of the column state with time by utilizing numerical integration. Here, the tray-by-tray dynamic material and energy balances are integrated until steady state. The temperature and the corresponding stoichiometric vapor phase on each tray are computed. This is a bubble point calculation and requires an iterative method. With the given pressure P and tray liquid composition $x_{j,i}$, the temperature T_j , and the vapor composition $y_{j,i}$ can be calculated by a Newton-Raphson iterative convergence method. Raoult's law states that the vapor pressure of a component in an ideal solution is equal to the vapor pressure of the pure component multiplied by its mole fraction, and the total vapor pressure of the solution is the sum of the vapor pressures of the individual components.

$$P = \sum_{i=1}^{NC} x_{j,i} P_{j,i(T)}^S \quad (3.5)$$

$$y_{j,i} = \frac{P_{j,i}^S}{P} x_{j,i} \quad (3.6)$$

The total and component mole balances throughout the column can be described by the following equations:

Column Base: $i = 1 : N_C$

$$\frac{dM_B}{dt} = L_1 - B - V_S \quad (3.7)$$

$$\frac{dx_{B,i}}{dt} = [L_1 x_{1,i} - B x_{B,i} - V_S y_{B,i}] / M_B \quad (3.8)$$

Trays: $i = 1 : N_C$ and $j = 1 : N_T$

$$\frac{dM_j}{dt} = L_{j+1} - L_j - r_j + \frac{\lambda}{\Delta H_V} r_j + F_j \quad (3.9)$$

$$\frac{dx_{j,i}}{dt} = [L_{j+1} x_{j+1,i} + V_{j-1} y_{j-1,i} - L_j x_{j,i} - V_j y_{j,i} + r_{j,i} + F_j z_{j,i}] / M_j \quad (3.10)$$

At both equations 3.9 and 3.10, the terms including reaction rate $r_{j,i}$ are omitted in the stripping section. In addition, F_j term is equal to zero throughout the column except the trays where the fresh streams are fed.

Reflux Drum: $i = 1 : N_C$

$$\frac{dM_D}{dt} = V_{NT} - R \quad (3.11)$$

$$\frac{dx_{NT,i}}{dt} = [V_{NT} y_{NT,i} - R x_{D,i}] / M_D \quad (3.12)$$

The vapor flow rate into the first tray, V_S , is the L_I fraction vaporized in the reboiler. The vapor flow rates on all trays of the column are consecutively calculated from stage 1 to stage N_T . The liquid molar flow rates of each tray of the column are respectively calculated from stage N_T to stage 2, using the material balance over each tray. Since equimolal overflow is assumed, the liquid and vapor rates are constant in the stripping section of the column. However, the liquid and vapor flow rates in the reactive section changes because of the following reasons: (i) the reaction is not equimolar (since two mole of reactants are consumed, while one mole product is produced) and (ii) the some of the liquid is vaporized due to the exothermic reaction. That is why vapor flow rate increases up and liquid flow rate decreases down through the reactive zone.

$$V_j = V_{j-1} - \frac{\lambda}{\Delta H_v} r_j \quad (3.13)$$

$$L_j = L_{j+1} - r_j + \frac{\lambda}{\Delta H_v} r_j \quad (3.14)$$

where λ is the heat of reaction and ΔH_v is the latent heat of vaporization. The reaction rate on tray j can be expressed in terms of mole fractions ($x_{j,i}$) and the kinetic holdups (M_j).

$$r_{j,i} = v_i M_j (k_{F_j} x_{j,A} x_{j,B} - k_{R_j} x_{j,C}) \quad (3.15)$$

where $r_{j,i}$ is the reaction rate of component i on the j th tray (mol/s), v_i is the stoichiometric coefficient which takes a negative value for the reactants, and M_j is the kinetic holdup on reactive tray j (mol). The kinetic holdup represents the amount of catalyst installed on a reactive stage.

The forward and backward specific rates following the Arrhenius law on tray j are given by

$$k_{F_j} = a_F e^{-E_F/RT_j} \quad (3.16)$$

$$k_{R_j} = a_R e^{-E_R/RT_j} \quad (3.17)$$

where a_F and a_R are the pre-exponential factors, E_F and E_R are the activation energies, and T_j is the absolute temperature on tray j .

The convergence method uses the following steps in the design procedure:

1. Fix the column pressure at a small value.
2. Fix the number of the reactive trays N_{RX} .
3. Fix the number of stripping trays N_S .
4. Fix the flow rate of the bottoms at 12.857 mol/s.
5. The flow rates of the fresh feed streams F_{0A} and F_{0B} depend on the amount of loss reactants at the bottoms stream. At each point in time during the simulation, the fresh feed flowrates are computed from the bottoms flow rate B and the value of the bottoms compositions $x_{B,i}$ that change by time until a steady-state solution is accomplished.

$$F_{0A} = 12.6 + Bx_{B,A} \quad (3.18)$$

$$F_{0B} = 12.6 + Bx_{B,B} \quad (3.19)$$

6. Manipulate the vapor boilup V_S with a P-only controller to control the level in the column base. There is no controller for the reflux drum level.
7. Manipulate the reflux flow rate with a PI controller to achieve the desired composition of product C in the bottoms.
8. By using bubble-point calculations, compute the temperatures and vapor compositions on each tray.
9. Compute the reaction rates using Equation 3.15 in the reactive zone.
10. By assuming equimolal overflow through the stripping section, compute the vapor flow rates and the liquid flow rates from Equation 3.13 and Equation 3.14, respectively.
11. Evaluate the time derivatives of the component material balances using equations 3.7-3.12.
12. Integrate all ODEs using the Euler algorithm.
13. Repeat from step 5 to step 12 until the desired steady-state solution is obtained.
14. Calculate total annual cost (TAC) of the RD column using the specified and calculated parameters.

15. Vary the number of the stripping trays over a range, and repeat steps 4-14 for each value of N_S .
16. Then, vary the number of the reactive trays over a range, and repeat steps 3-15.
17. Finally, vary the value of the column pressure over a wide range, and repeat steps 2-16 for each pressure value. Select the design with the minimum TAC as the economically optimum steady-state design.

3.4. Sizing and Economics

To find the economically optimum steady-state design, total annual cost (TAC) is used as the objective function that sums the energy and capital costs of the system assuming a payback period (β_{pay}) of 3 years for capital cost. Total annual cost is given by

$$TAC = \text{Energy Cost} + \frac{\text{Capital Investment}}{\beta_{\text{pay}}} \quad (3.20)$$

The energy and the capital costs of the process are calculated using the following equations [50].

$$\text{Column cost} = 17640 D_C^{1.066} L_C^{0.802} \quad (3.21)$$

$$\text{Tray cost} = 229 D_C^{1.55} N_T \quad (3.22)$$

$$\text{Heat exchanger cost} = 7296 (A_R^{0.65} + A_C^{0.65}) \quad (3.23)$$

$$\text{Energy cost} = 0.6206 \Delta H_V V_S \quad (3.24)$$

To calculate the terms in the TAC equations, following set of equations taken from Kaymak and Luyben's paper are used [15].

- (i) The diameter of the column is calculated from the equation

$$D_C = 1.735 \times 10^{-2} \left(\frac{M_W T}{P} \right)^{0.25} V_{NT}^{0.5} \quad (3.25)$$

- (ii) The column height is calculated assuming a 0.61-m (2-ft) tray spacing and allowing 20% more height for base-level volume.

$$L_C = 0.73152 N_T \quad (3.26)$$

- (iii) The heat-transfer areas of the reboiler and condenser are calculated using the steady-state vapor flow rates and the heat of vaporization.

$$A_R = 0.0042 \frac{V_S \Delta H_V}{U_R \Delta T_R} \quad (3.27)$$

$$A_C = 0.0042 \frac{V_{NT} \Delta H_V}{U_C \Delta T_C} \quad (3.28)$$

The vapor flow rate in the top tray, V_{NT} , is higher than the vapor flow rate in the reboiler, V_S , because of the liquid vaporized through the reactive section. Thus, the heat-transfer areas of the reboiler and condenser are calculated using two different vapor rates.

- (iv) The process is assumed to be equally reliable and to operate for 365 days per year.

3.5. Process Control

The control objective is to maintain the bottoms product purity within a desired range in the face of the load disturbances, which are production rate changes and feed composition variations. Composition analyzers can be used to control the product purities of RD columns. However, direct composition measurements are expensive, unreliable and involve large dead-times in the control loops. Therefore, inferential variables such as tray temperatures are used to infer the product composition instead of direct composition measurement in RD columns. As Marlin states, although it is not always impossible, automated control is difficult because of the lack of measurements of key variables in a timely manner. To improve this situation inferential control uses extra information. Here, the extra information is additional measured variables that, while not giving a perfect indication of the key unmeasured variable, provide a valuable inference [48].

There are six control valves associated with the RD column, as shown in Figure 3.1. Therefore, there are six control degrees of freedom. Three of them are used for inventory control and pressure control in all control schemes investigated in this study. Reflux drum level and base level are controlled by manipulating reflux flow rate and bottoms flow rate, respectively. Column pressure is controlled by manipulating cooling water of condenser. Two of the remaining three valves can be

used to control two tray temperatures. Therefore, three different types of two-temperature inferential control structures are possible for this column configuration. All structures consist of multi-loop SISO (single input-single output) controllers where one controlled variable paired with one manipulated variable. Figure 3.4 shows the block diagram of a feedback control loop.

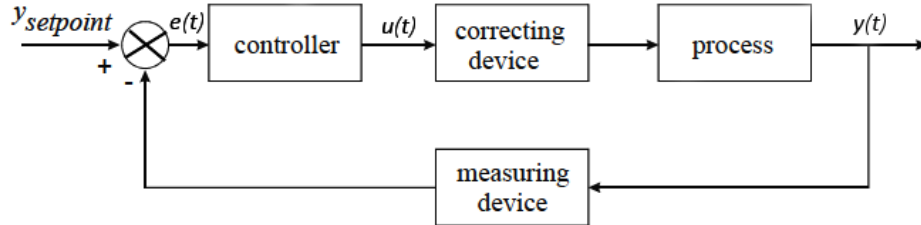


Figure 3.4: A Feedback Control Loop

The output $y(t)$ is a tray temperature or liquid level. The measuring device or sensor measures the value of the output variable. The value of the process measurement is compared with a set point (target value) and subtracted from it. The difference or error serves as input to a controller. The controller calculates a change of the signal for the control valve. The correcting device adjusts the corresponding flow rate. Conventional linear PI controllers are used in temperature control loops. The PI controllers solve the following equation [49]:

$$u(t) = K_C \left[e(t) + \frac{1}{\tau_I} \int e(t) dt \right] \quad (3.29)$$

where K_C is the controller gain, τ_I is integral (or reset) time, u is the control signal and e is the control error $e (y_{sp} - y)$.

Both level controllers in the structure are P-only controllers. The describing equation is

$$u(t) = K_C e(t) \quad (3.30)$$

3.5.1. Control Structure CS1

Figure 3.5a shows the first control structure CS1 in which the fresh feed stream F_{0A} and vapor boilup V_S are manipulated by two temperature controllers. The heavy reactant fresh feed stream F_{0B} is flow controlled and serves as the production rate handle. Feed ratio control CS1-FR examined as a second version of CS1 is given in

Figure 3.5.b. The light reactant fresh feed is ratioed to the heavy reactant feed. The ratio is set by a temperature controller. The heavy reactant fresh feed stream F_{0B} serves as the production rate handle and is flow controlled as well.

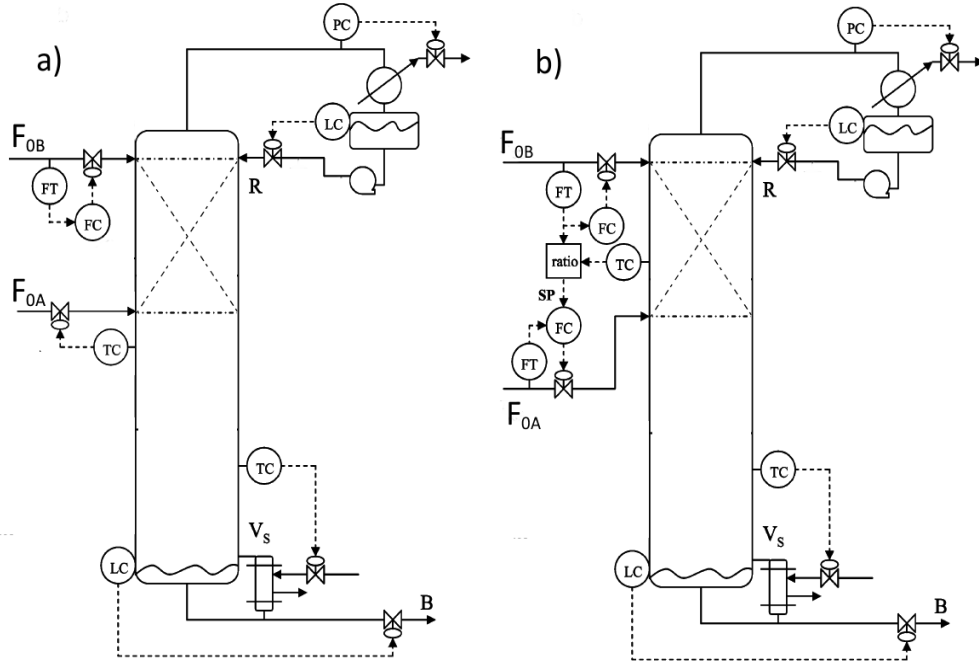


Figure 3.5: Control Structures: a) CS1 b) CS1-FR

3.5.2. Control Structure CS2

Figure 3.6 gives the second control structure in which two temperature controllers manipulate the fresh feed stream F_{0B} and the vapor boilup V_s to maintain the temperatures on two trays. The throughput is set by flow controlling the fresh feed of F_{0A} .

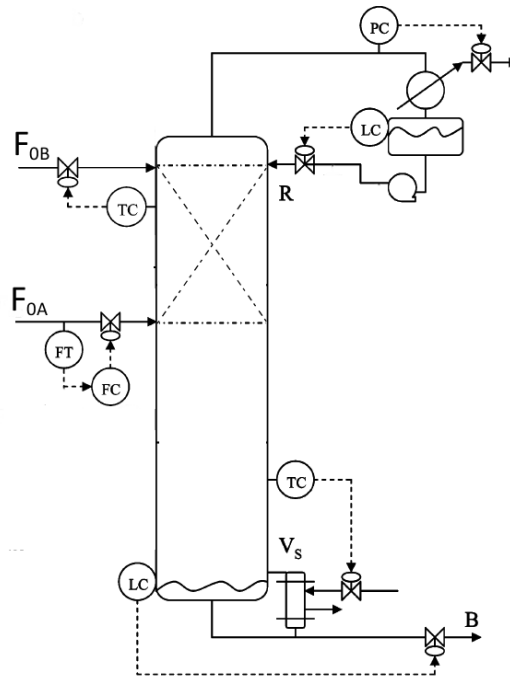


Figure 3.6: Control Structure CS2

3.5.3 Control Structure CS3

Control structure CS3 is given in Figure 3.7, where two temperature controllers manipulate two fresh feed streams to maintain the temperatures of two trays. In this case, the vapor boilup is the production-rate handle and is flow controlled.

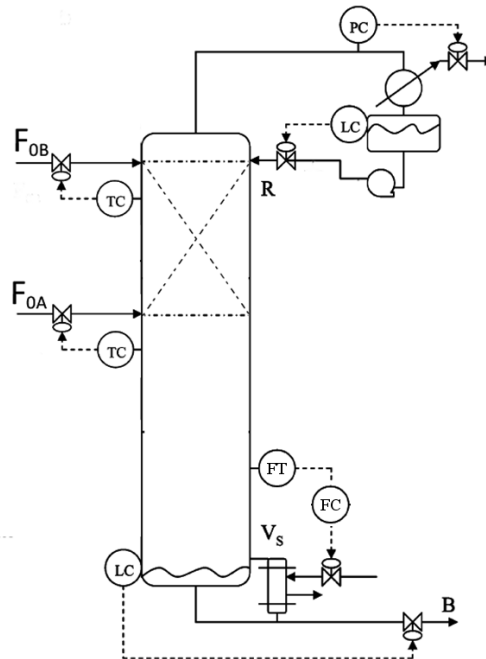


Figure 3.7: Control Structure CS3

3.5.6. Selection of Temperature Control Trays

A procedure consisting of two methods are performed to find which trays should be selected to apply the inferential control. A dynamics response analysis (sensitivity analysis) is applied as the first part of the procedure. Sensitivity analysis is used to find the steady-state gains of the column in the face of small changes in the manipulated variables [50]. While the input is changed in small positive and negative steps, the corresponding output responses to these steps are observed. Therefore, the change in tray temperature is rationed to the change in the manipulated variable. That gives the open-loop steady-state gain between tray temperatures and manipulated variable. The tray having the largest temperature change is the most sensitive tray, and selected to be controlled. To support the obtained sensitivity analysis results, singular value decomposition (SVD) method is used to select the most sensitive trays to be controlled by using the steady-state gains. SVD is a method for identifying and ordering the dimensions along which data points exhibit the most variation [51]. To perform an SVD method, a gain matrix K_p having N_T rows (the number of trays) and two columns (the number of manipulated variables) are formed. This matrix is broken down by using standard SVD into the product of three matrices; a left singular vector matrix U , a diagonal matrix of singular values Σ , and the right singular vector matrix V . The method is usually expressed as:

$$K_p = U \Sigma V^T \quad (3.31)$$

The columns of U matrix are plotted versus trays. The largest elements of columns indicate the tray locations which are the most sensitive to input changes applied and can be effectively controlled [52,53].

3.5.7. Controller Tuning

In 1984, Astrom and Hagglund presented a relay feedback system to generate sustained oscillation for controller tuning [54]. Many researches on extending and modifying the relay feedback auto-tuning method have been reported in recent years [55-57]. The relay feedback test identifies two important parameters for controller tuning, the ultimate gain and ultimate period. This test is based on the observation that a closed-loop system in which the output lags (y) behind the input (u) by π radians may oscillate with the period P_u under relay control. The relay controller is a

simple on-off controller. The block diagram of a relay feedback system is shown in Figure 3.8.

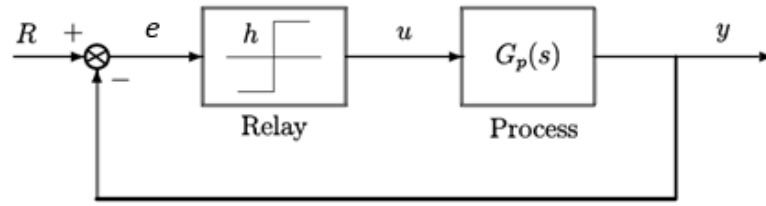


Figure 3.8: Block Diagram of a Relay Feedback System

The relay controller has a specified amplitude h and a time delay. A relay with the specified amplitude is inserted in the feedback loop. Initially, the input $u(t)$ becomes $+h$ as shown in Figure 3.9. As the output $y(t)$ starts increasing after the dead time (D), the relay switches to the opposite direction, $u(t) = -h$. Since there is a phase lag of $-\pi$, a limit cycle with a period is generated. The period of the limit cycle is the ultimate period, P_u . From the principle harmonic approximation of the oscillations, the ultimate gain (K_u) can be approximated as

$$K_u = \frac{4h}{\pi a} \quad (3.32)$$

where h is the relay amplitude and a is the amplitude of oscillation [55-57].

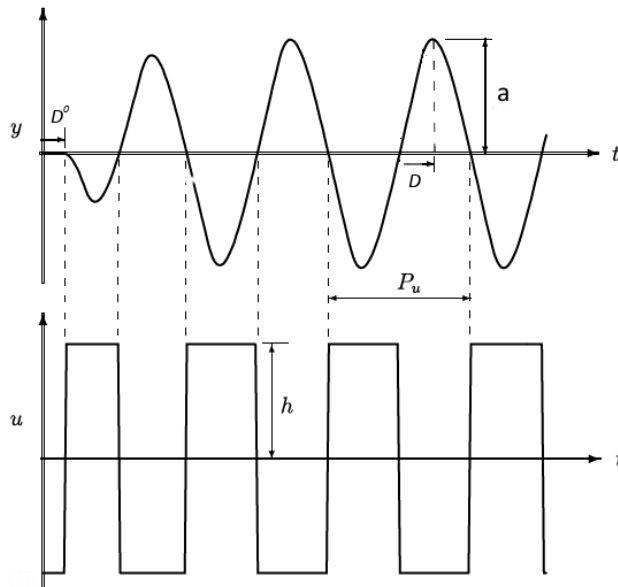


Figure 3.9: Typical Relay Feedback Response

Using the ultimate gain K_u and the ultimate period P_u obtained from the relay feedback test, controllers for the temperature loops are tuned using Tyreus-Luyben tuning method [58].

$$K_c = \frac{K_u}{3.2} \quad (3.33)$$

$$\tau_I = 2.2P_u \quad (3.34)$$

Two first-order measurement lags with a time constant of 60 s each are used in temperature loops. Temperature transmitter spans of 100 K are used for dimensionless controller gains. To get a faster closed-loop response while avoiding large oscillations, a detuning factor f is used in some temperature loops. The detuning factor is obtained empirically.

$$K_c = \frac{K_u}{3.2 \times f} \quad (3.35)$$

$$\tau_I = 2.2P_u \times f \quad (3.36)$$

The base and reflux drum levels are controlled by P-only controllers with a gain of 2. All valves are designed to be half open at steady state.

4. RESULTS AND DISCUSSIONS

4.1. Effect of Design Variables

Design variables have been examined to find optimum designs of the ternary RD process. The detailed results are given just for the base case, $\alpha_{390} = 2$. Figure 4.1 shows the impact of design variables for ternary RD process. The left column graphs in Figure 4.1 shows the effect of number of stripping trays, while number of reactive trays is kept constant at 5. It is demonstrated that the increase in the number of stripping trays decreases the vapor boilup. Despite the decreasing vapor boilup, adding more stripping trays increases the capital cost. The change in the number of reactive trays is given on the right column graphs of Figure 4.1, where the number of stripping trays is kept constant at 13. It is demonstrated that having too few reactive trays increases the vapor boilup to obtain desired product purity. However, adding more reactive trays increases the capital cost. As the result of the tradeoff between energy and capital costs, it is found that there is an optimum tray number for the ternary RD column.

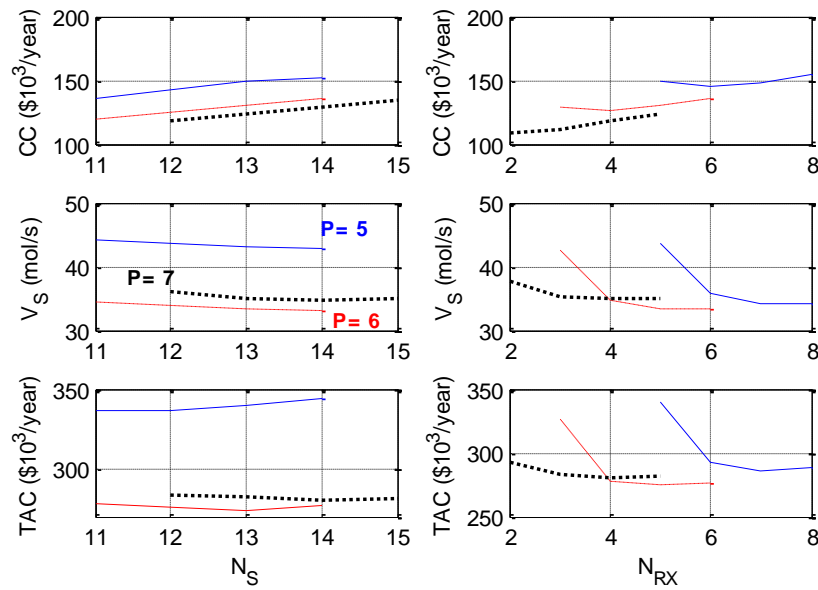


Figure 4.1: Effect of Design Variables

Figure 4.2 gives the effect of changing column pressure on temperature profiles. Since operating pressure affects the temperature of the reactive zone, there is an optimum pressure. High column pressures cause an increase in the temperature of the reactive section. Although high temperatures increase the specific reaction rates, they drop the chemical equilibrium constants because of the exothermic reaction system. That is, the reaction yield decreases in high temperatures of the reactive zone. On the other hand, low column pressures give lower temperatures declining specific reaction rates. Therefore, both for high and low pressures, the column requires higher vapor heat input to obtain desired product impurity.

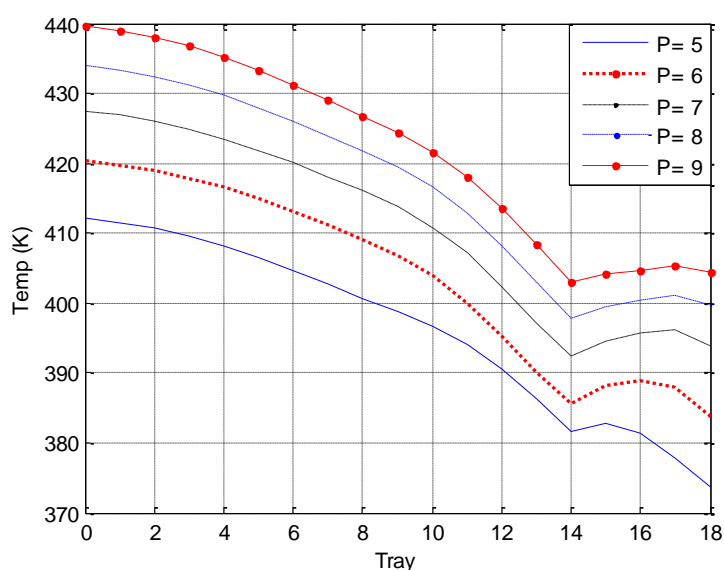


Figure 4.2: Effect of Pressure on Temperature Profiles

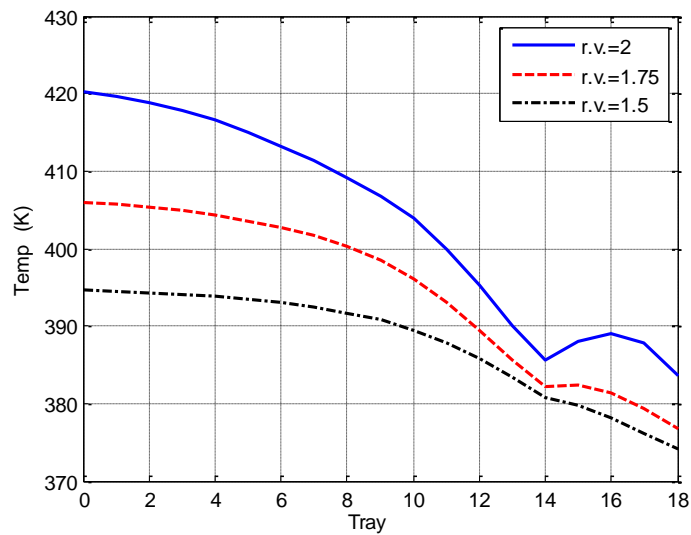
4.2. Effect of Relative Volatility

First, the effect of relative volatility on the base case configuration has been investigated. The optimum column design for $\alpha_{390} = 2$ case is taken as the base case configuration. The optimum results of this configuration for different α_{390} values are given in Table 4.1. Since the separation gets more difficult as the relative volatilities get closer, the system needs more vapor boilup. Thus, the energy cost increases as the result of the increase in the vapor boilup. Moreover, the column diameter and the heat transfer areas of reboiler and condenser increase as the result of the increasing vapor boilup. Therefore, the capital cost increases when relative volatilities get closer. That is why the total annual cost increases as the relative volatilities get closer.

Table 4.1: Results of the Base Case

	α_{390}		
	2	1.75	1.5
Design Parameters			
N_S	13	13	13
N_{RX}	5	5	5
P(bar)	6	6	6
F_{0A} (mol/s)	12.60	12.60	12.60
F_{0B} (mol/s)	12.857	12.857	12.857
V_S (mol/s)	33.45	47.15	85.89
R (mol/s)	51.60	65.30	104.03
Dc (m)	0.93	1.05	1.32
CE (\$10 ³ /year)	144.1	203.1	370.1
CC (\$)	395.3	463.7	631.3
TAC (\$10 ³ /year)	275.9	357.7	580.5

Figure 4.3 shows the effect of relative volatilities on temperature profiles for the base case configuration. As the relative volatilities get closer, the average temperature of the column decreases. In addition, temperature profile in reactive section becomes linear.

**Figure 4.3:** Effect of Relative Volatility on Temperature Profile

Secondly, the effect of relative volatility on the optimum column configurations has been investigated. Optimum designs of all relative volatility cases are summarized in Table 4.2. As the relative volatilities get closer, separation gets more difficult. Thus, RD column requires more separation trays and vapor boilup. The decrease in the

average reactive zone temperature results in a decrease of specific reaction rates. Therefore, trays that are more reactive are required at the relative volatility of 1.5 as shown in Figure 4.4. As the result, TAC of the column increases as the temperature dependence of the relative volatilities increases.

Table 4.2: Results of the Optimum Designs

	α_{390}		
	2	1.75	1.5
Design Parameters			
N_S	13	18	20
N_{RX}	5	5	9
P(bar)	6	7	6
F_{0A} (mol/s)	12.60	12.60	12.60
F_{0B} (mol/s)	12.857	12.857	12.857
V_S (mol/s)	33.45	41.12	51.77
R (mol/s)	51.60	59.26	69.91
Dc (m)	0.93	0.97	1.09
CE (\$10 ³ /year)	144.1	177.1	223.2
CC (\$10 ³)	395.3	459.7	559.1
TAC (\$10 ³ /year)	275.9	330.4	409.7

Figure 4.4 shows the effect of relative volatilities on temperature profiles for the optimum column configurations. The sharpness of the temperature profile in the stripping section decreases, as the relative volatilities get closer. Thus, the temperature range between bottoms and reflux drum decreases.

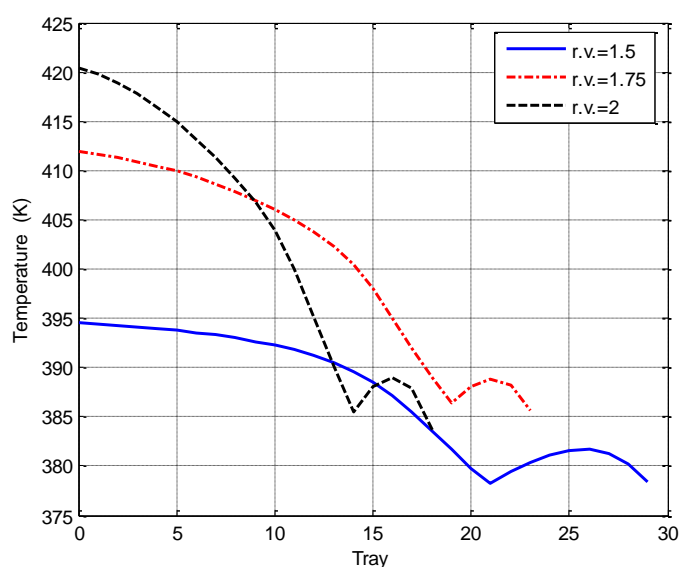


Figure 4.4: Temperatures Profiles for Optimum Designs for Three Different Cases

Figure 4.5 shows the composition profiles of the optimum designs for three different relative volatility cases. The highest composition of reactant A is at the reflux drum because reactant A is the lightest component in RD column. The other reactant B has its highest composition at the top of reactive zone which is also its feed tray. While the composition of product C increases down through the stripping section, the composition of reactant A decreases.

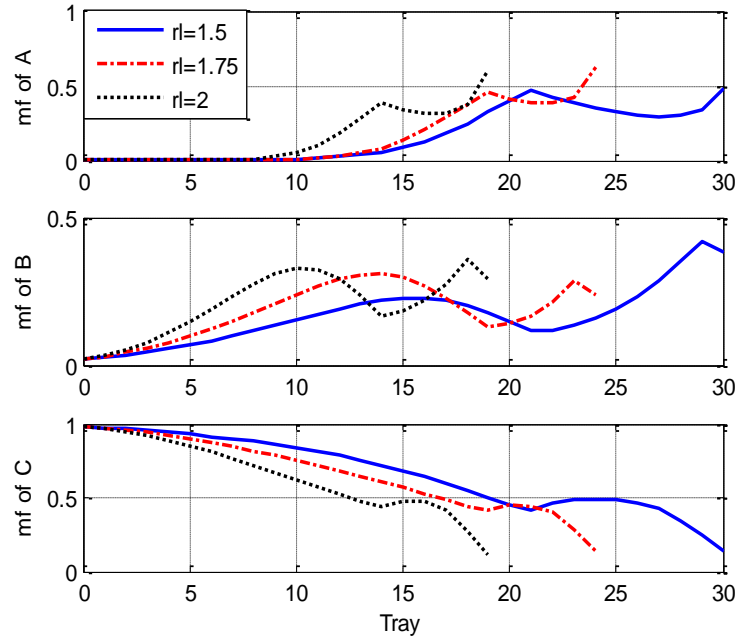


Figure 4.5 : Compositions of Profiles of Optimum Designs for Three different Cases

4.3. Controllability of Base Case Design for Different Relative Volatility Cases

4.3.1. Control Structure CS1

Figure 4.6 shows the steady-state gains and SVD results for base case designs. The graphs on the first row show the sensitivity analysis, while the ones on the bottom row give the SVD results. The steady state gains between tray temperatures and the fresh feed stream F_{0A} are negative. Having the biggest gains K_{F0A} in the stripping section indicates that the trays in this section have higher sensitivity to the changes in input F_{0A} . On the other hand, the most sensitive trays are at the top of the reactive zone for the second input V_S . Moreover, the steady state gains between the tray temperatures and vapor boilup are positive. The SVD analysis results support the sensitivity analysis results for all relative volatility cases. The SVD analysis for the base case suggests that the temperature of tray 4 in the stripping section should be

controlled by manipulating the fresh feed flow rate F_{0A} , while the temperature of tray 18 in the reactive section should be controlled by manipulating the vapor boilup V_S for control structure CS1. As the relative volatilities decrease, the sensitivity of trays for F_{0A} gets smaller and the place of the most sensitive tray shifts towards reactive section. On the other hand, no gradually change is observed in the magnitude of steady-state gains for V_S . It is seen that tray 17 is the most sensitive tray for V_S at the relative volatilities 1.75 and 1.5.

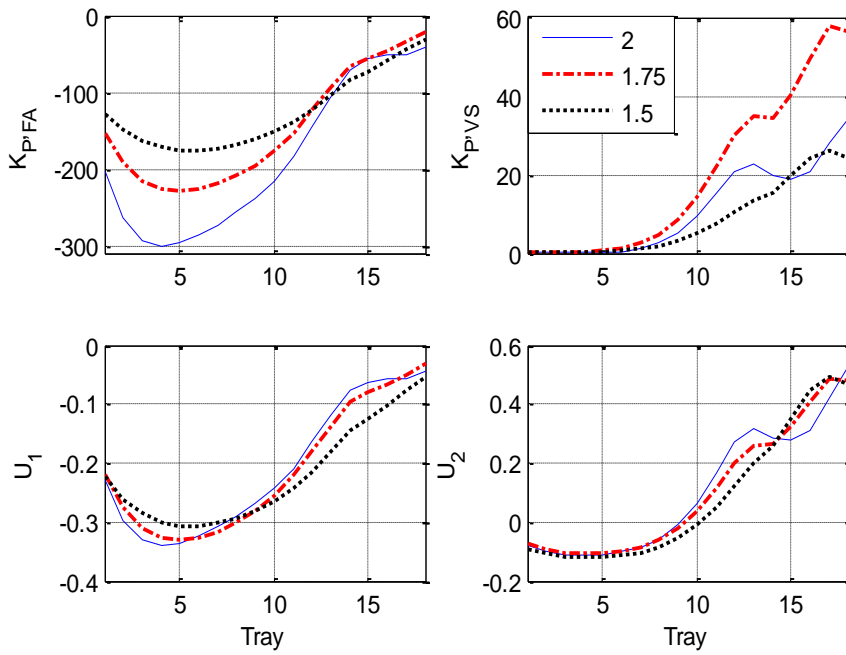


Figure 4.6: Steady-State Gains and SVD Analysis Results

Controller parameters calculated for CS1 are given in Table 4.3 for all relative volatility cases.

Table 4.3 : Tuning Parameters of CS1

Design	α_{390}	Control Loop	K_U	P_U (min)	K_C	τ_I (min)	F
13/5	2.00	$F_{0A} - T_4$	53.05	7.62	16.58	16.764	1
		$V_S - T_{18}$	13.49	36.42	4.22	80.124	1
1.75	1.75	$F_{0A} - T_5$	63.66	8.4	19.89	18.48	1
		$V_S - T_{17}$	39.79	8.22	12.43	18.084	1
1.50	1.50	$F_{0A} - T_6$	121.26	6.96	37.89	15.312	1
		$V_S - T_{17}$	475.09	2.16	49.49	14.256	3

Figure 4.7 shows the closed-loop responses of control structures CS1 and CS1-FR to a positive 20% step change in the production rate handle, F_{0B} . The systems shut down in the face of this disturbance for all the relative volatility cases.

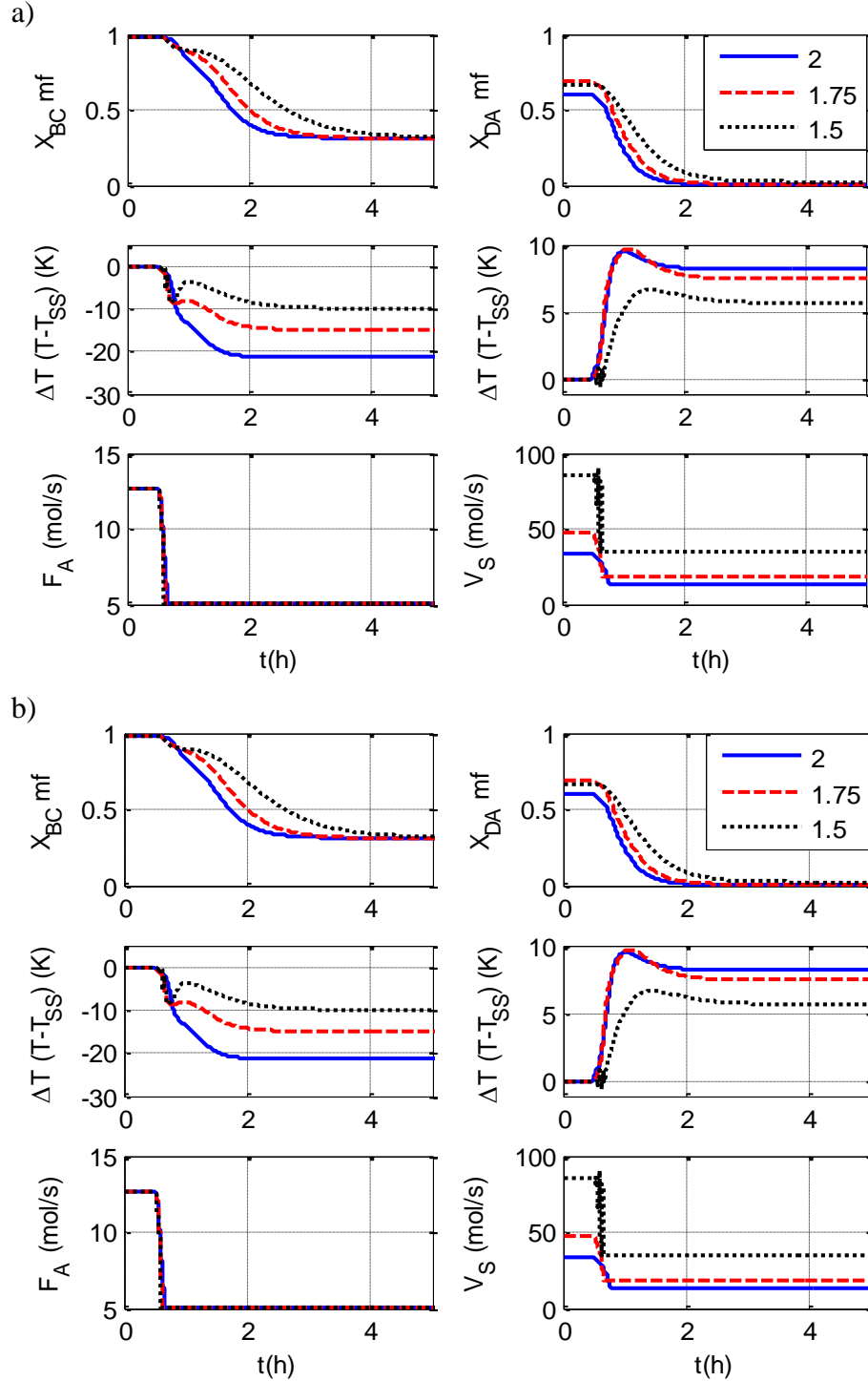


Figure 4.7: Results of a) CS1 b) CS1-FR for +20% F_{0B} Step Change

Figure 4.8 plots the steady state variation in the controlled reactive tray temperature T_{18} with respect to F_{0A} , F_{0B} and V_S for the base case. The steady state variations are

negative for the increase of F_{0A} , and positive for the decrease of F_{0A} . Similarly, the increase of F_{0B} increases the temperature of tray 18, while the decrease of F_{0B} decreases the temperature of tray 18 as expected. However, this tray temperature exhibits an open-loop input multiplicity with respect to V_S . This is illustrated in Figure 4.8 that plots input output relations exhibiting process gain reversal. A cross-over slope for a large increase in V_S occurs, which is opposite the base-case slope. This multiplicity shows that the system is highly nonlinear, and this can cause wrong control action or steady state transition [41-45]. Thus, it is claimed that the fail of the control structure is because of this wrong action problem. Because of step change, the system is pushed towards the input multiplicity region, resulting with wrong control action as suggested by the input output relations.

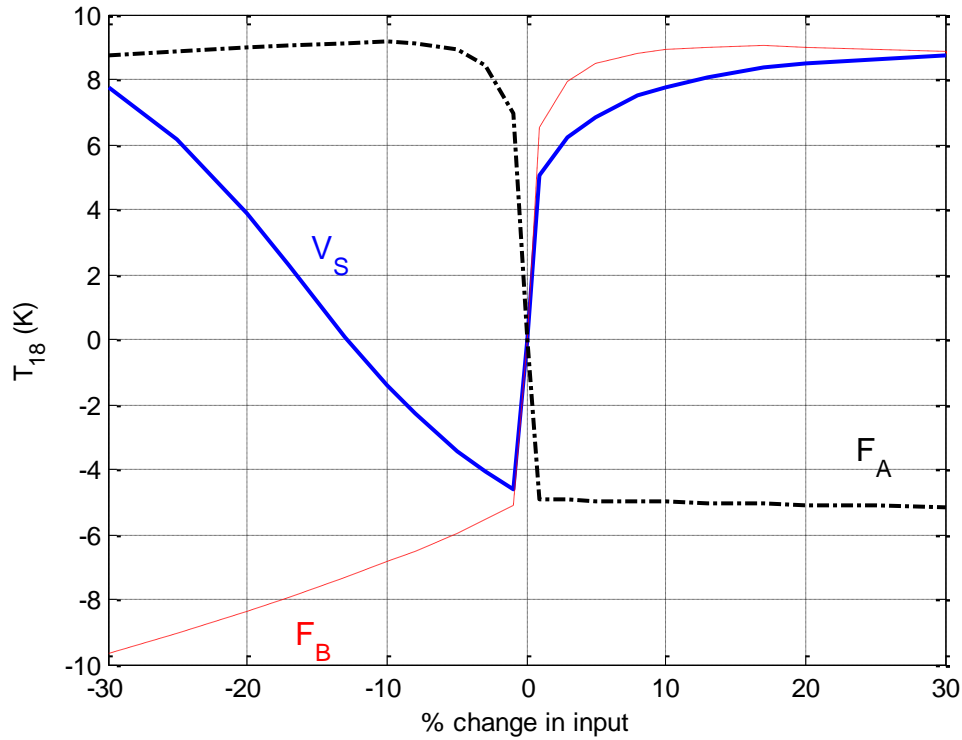


Figure 4.8 : Steady State Variation in Controlled Reactive Tray Temperature T_{18}

4.3.2. Control Structure CS2

The manipulated variables for CS2 are the fresh feed stream F_{0B} and the vapor boilup V_S . Figure 4.9 shows the steady-state gains and SVD analysis results for three case studies. While the graphs on the first show the sensitivity analysis results, the bottom row includes the SVD analysis results. Results show that the steady state gains K_{F0B}

and K_{VS} are positive and their characters are very similar. It is seen that the top tray of the reactive section is the most sensitive tray for both manipulated variables F_{0B} and V_S . The SVD analysis results also support the sensitivity analysis results. The control loops and related PI controller parameters are given in Table 4.4.

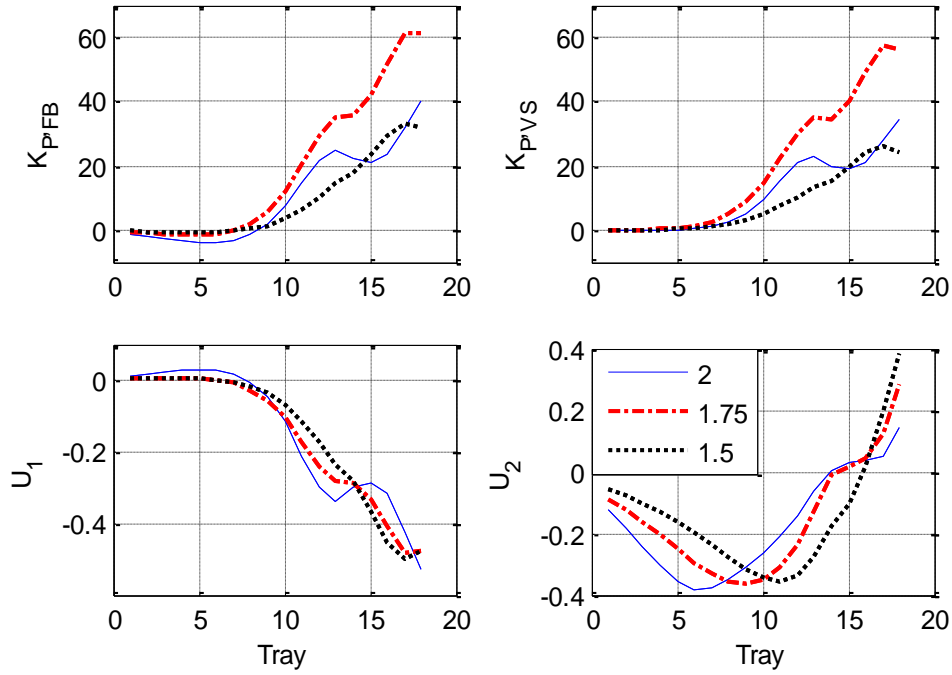


Figure 4.9: Steady-State Gains and SVD Analysis

Table 4.4 : Tuning Parameters of CS2

Design	α_{390}	Control Loop	K_U	P_U (min)	K_C	τ_I (min)	F
13/5	2	$F_{0B} - T_{18}$	125.07	3.42	39.08	7.524	1
		$V_S - T_{17}$	23.58	15.48	7.37	34.056	1
	1.75	$F_{0B} - T_{18}$	293.37	2.7	91.68	5.94	1
		$V_S - T_{17}$	39.79	8.22	12.43	18.084	1
	1.5	$F_{0B} - T_{18}$	573.53	2.7	179.23	5.94	1
		$V_S - T_{17}$	475.09	2.16	49.48	12.96	3

Figure 4.10 shows the closed loop responses of the control structure for $\pm 20\%$ step changes in the production rate handle, F_{0A} . Although both controlled temperatures turn back to their set points by manipulating F_{0A} and V_S , the purity of the bottoms product settles down to a new steady state.

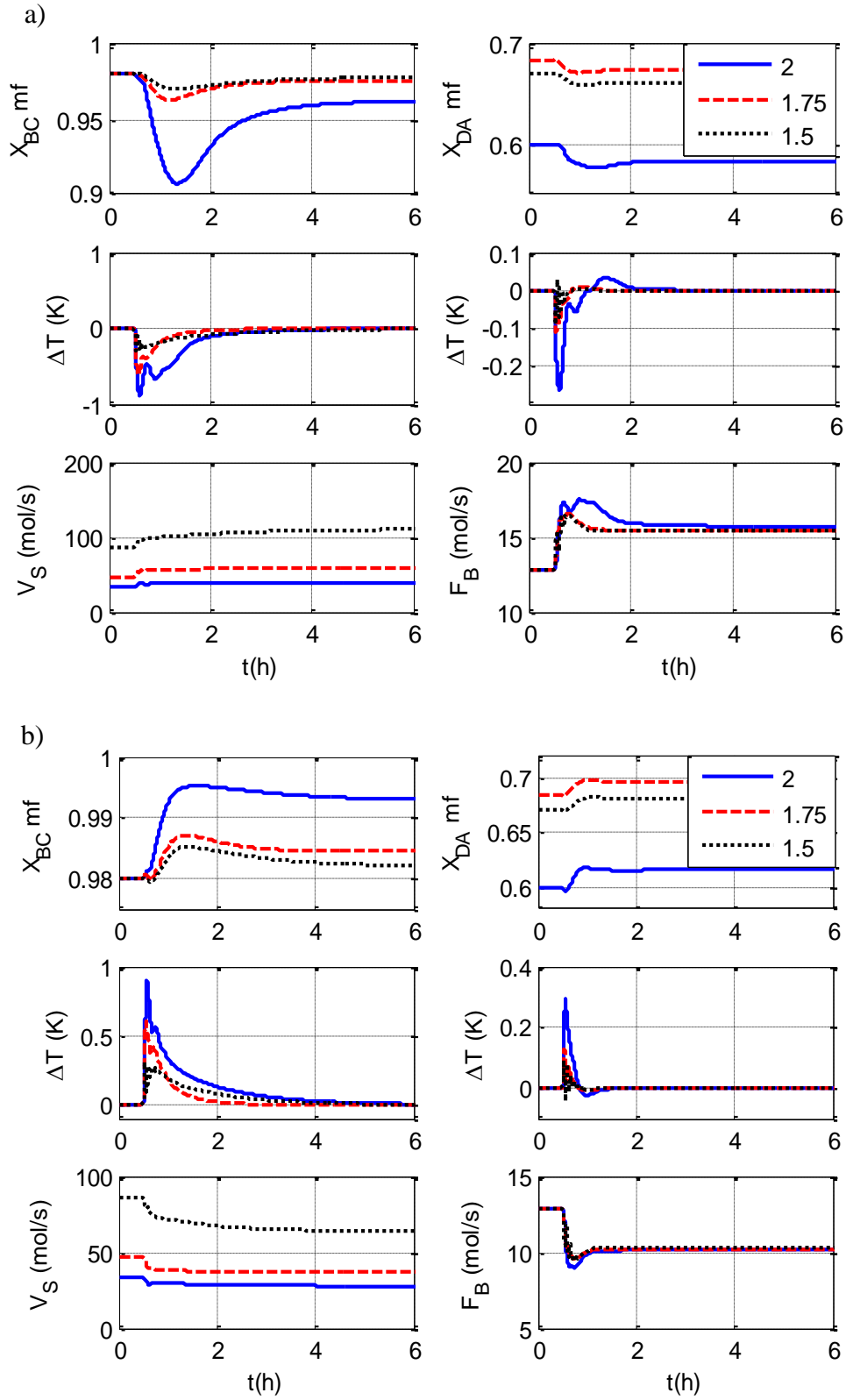


Figure 4.10: Results of Control Structure CS2: a) +20% F_{0A} , b) -20% F_{0A}

Figure 4.11 compares the difference between the two fresh feed flow rates for $\pm 20\%$ throughput changes for the base case. It is seen that these disturbances effect stoichiometric feed balance. As the result of this balance problem, there is not enough reactant A to prevent the heavy reactant B from the reaction section into the stripping section. Therefore, the impurity of B in the bottoms stream increases and the product purity (and conversion) converges to a different value than the initial steady state value.

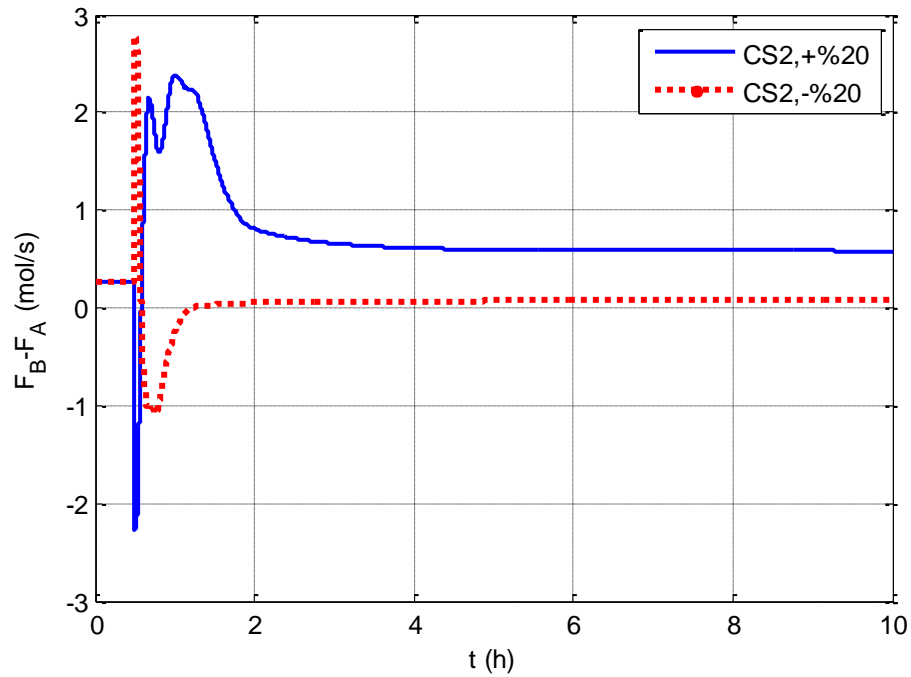


Figure 4.11: The Transient Stoichiometric Imbalance ($F_{0B} - F_{0A}$) for the Base Case

4.3.3. Control Structure CS3

Figure 4.12 shows the steady-state gains and SVD analysis. The graphs at the top row show the sensitivity analysis, and the bottom ones give SVD analysis. According to the results, the most sensitive trays are in the stripping section for the fresh feed flow rate of F_{0A} , while the most sensitive trays are at the top of the reactive zone for the fresh feed flow rate of F_{0B} . The SVD analysis supports the sensitivity analysis results. As the relative volatilities decrease, the sensitivity of trays paired with F_{0A} gets smaller. However, the relative volatility does not affect the location of the most sensitive trays. The control loops and PI controller parameters are given in Table 4.5.

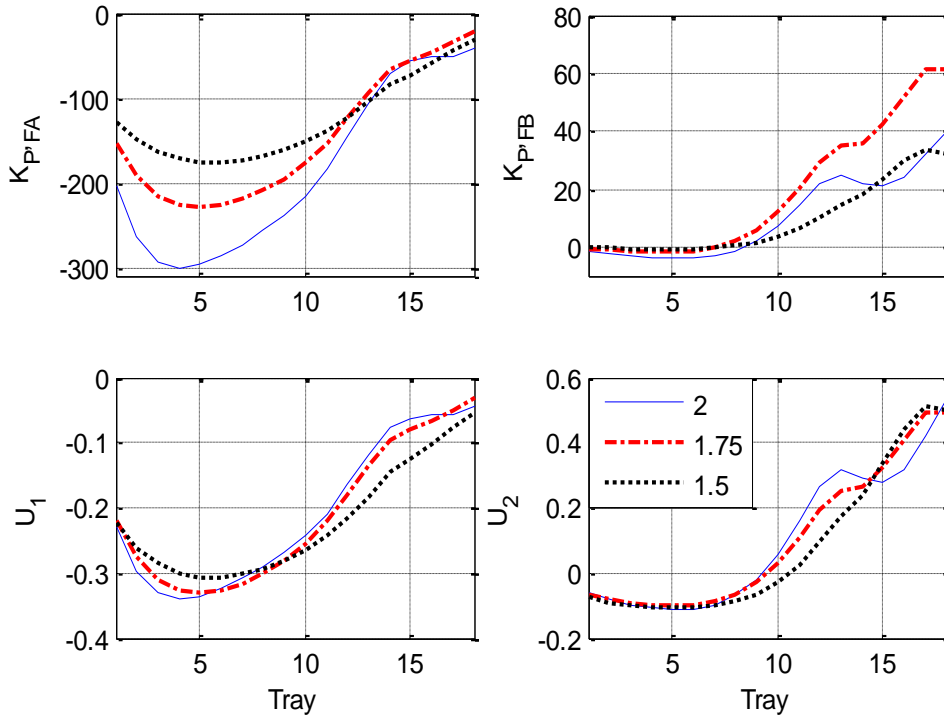


Figure 4.12 : Steady-State Gains and SVD Analysis

Table 4.5 : Tuning Parameters of CS3

Design	α_{390}	Control Loop	K_U	P_U (min)	K_C	τ_I (min)	F
13/5	2	$F_{0A} - T_4$	53.05	7.62	16.58	16.764	1
		$F_{0B} - T_{18}$	125.07	3.42	13.03	22.572	3
	1.75	$F_{0A} - T_5$	63.66	8.4	9.95	36.96	2
		$F_{0B} - T_{17}$	89.16	5.04	9.29	33.264	3
	1.5	$F_{0A} - T_6$	121.26	6.96	37.89	15.312	1
		$F_{0B} - T_{17}$	81.1	10.02	8.45	66.132	3

Figure 4.13 and Figure 4.14 give the closed loop responses of control structure CS1 for the base case designs. In Figure 4.13A, the disturbance is a positive 20% step change in the production rate handle, V_S . Figure 4.13B gives the results for a negative 20% step change in V_S . Figure 4.14A shows the closed loop response when the composition of the fresh feed F_{0A} is changed from pure A ($z_{0A(A)} = 1$) to a mixture of A and B ($z_{0A(A)} = 0.95$ and $z_{0A(B)} = 0.05$). Figure 4.14B gives the closed loop response when the composition of the fresh feed F_{0A} is changed from pure A ($z_{0A(A)} = 1$) to a mixture of A and C ($z_{0A(A)} = 0.95$ and $z_{0A(C)} = 0.05$).

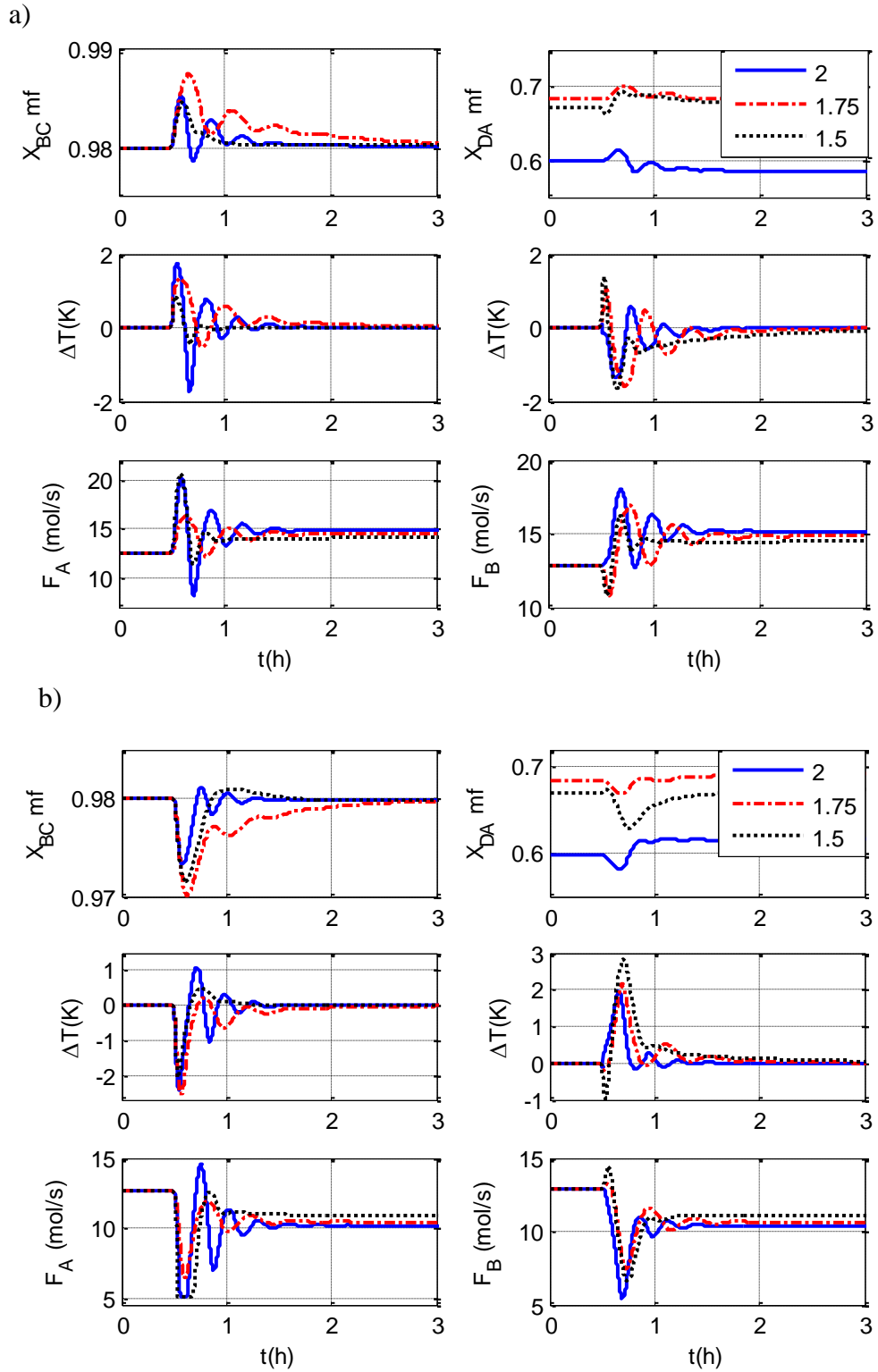
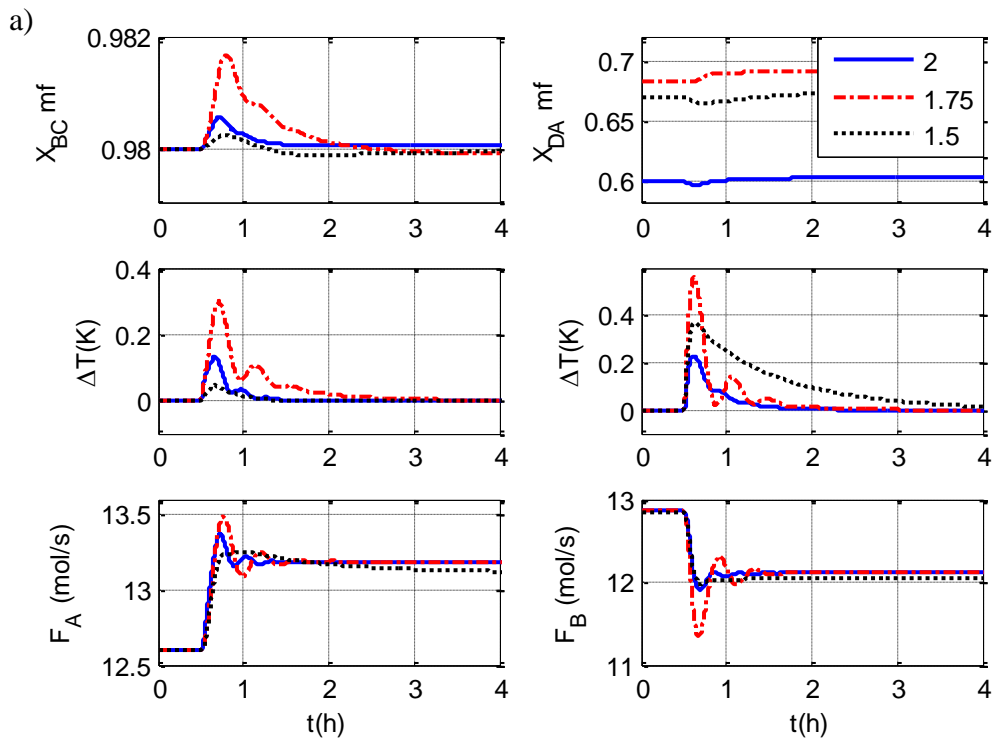


Figure 4.13: Result of Control Structure CS3: a) +20% VS b) -20% VS

Although the manipulated fresh feed streams have opposite actions, the systems are dynamically stable, and the control structure CS3 successfully provides column regulation for a wide range of disturbances. The column settles down to the final steady state within 3 h.

Since this control structure works well, in spite of the opposite actions of temperature controller loops, it deserves a closer look. An increase in the vapor boilup results in an initial increase of the temperature of both control trays (trays 4 and tray 18). Temperature controller of tray 4 has a direct action, so it increases the F_{0A} feed flow rate. However, temperature controller of tray 18 has a reverse action, and it decreases the F_{0B} flow feed flow rate. This change corresponds to an increase in the amount of reactant A. This excess reactant A starts to move up through the column. Since there is no distillate stream in this configuration, all light reactant A moving up turns back to the column by the reflux, which decreases the temperatures at the top of the reactive section. Therefore, temperature controller of tray 18 starts to increase the F_0 flow rate. Finally, the fresh feed streams settle down to new steady state values providing a precise balance of stoichiometry.



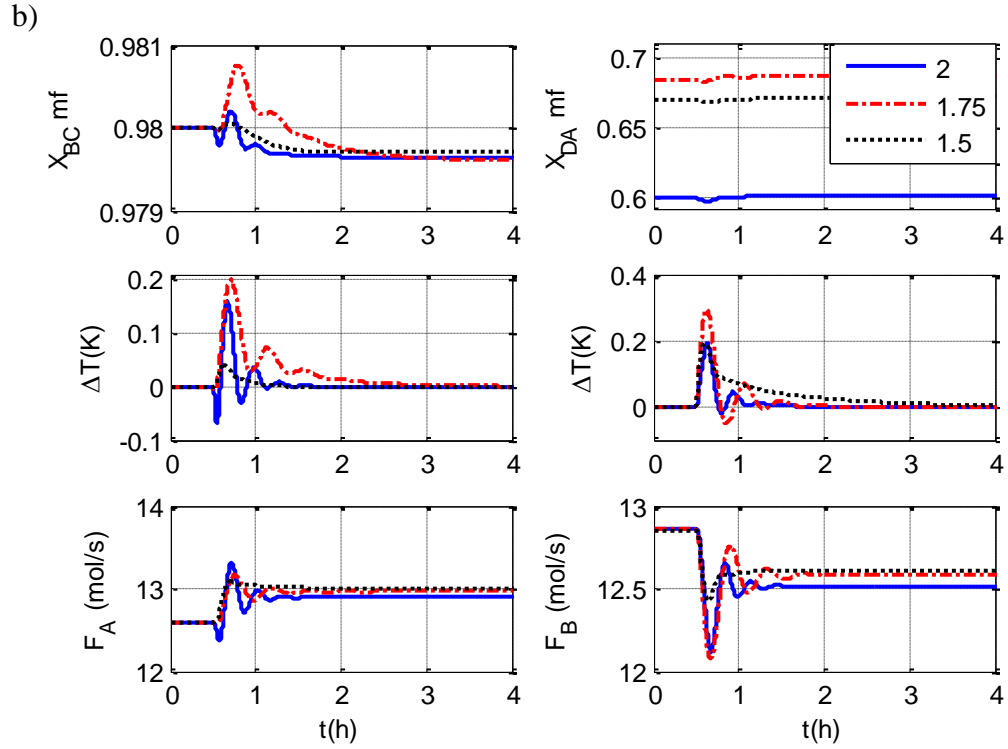


Figure 4.14: Result of Control Structure CS3: a) $z_{0A(B)} = 0.05$, and b) $z_{0A(C)} = 0.05$

4.4. Controllability of Optimum Designs for Different Relative Volatility Cases

4.4.1. Control Structure CS1

Figure 4.15 shows the results of the steady-state gains and SVD analysis for the optimum designs of different relative volatility cases. According to the results, the most sensitive trays to the changes in fresh feed flow rate F_{0A} are in the stripping section, while the most sensitive trays are at the top of the reactive zone for the flow rate of V_s . The SVD analysis results for both manipulated variables support the sensitivity analysis results. It is seen that the sensitivity of trays for F_{0A} gets smaller as the relative volatilities decrease. On the other hand, the magnitudes of steady state gains for V_s increase when relative volatility changes from 2 to 1.75, while they decrease with the decrease of relative volatility to 1.5. The control loops and PI controller parameters are given in Table 4.6 for each design.

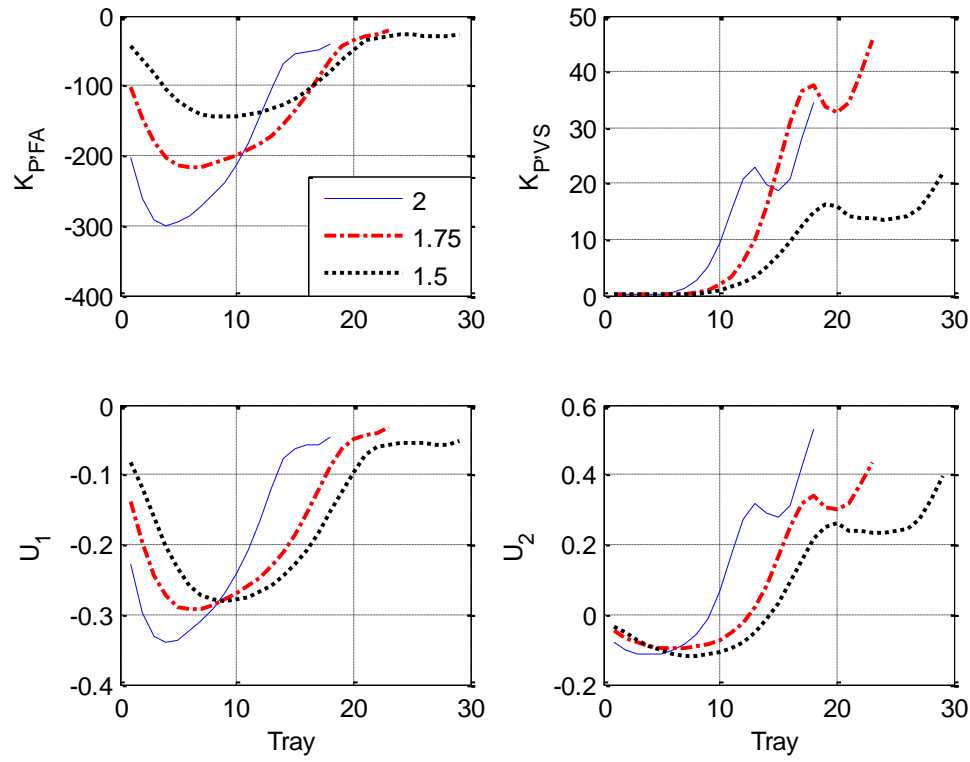


Figure 4.15 : Steady-State Gains and SVD Analysis

Table 4.6 : Tuning Parameters of CS1

Design	α_{390}	Control Loop	K_U	P_U (min)	K_C	τ_1 (min)	F
13/5	2	$F_{0A} - T_4$	53.05	7.62	16.58	16.764	1
		$V_S - T_{18}$	13.49	36.42	4.22	80.124	1
18/5	1.75	$F_{0A} - T_6$	63.66	8.4	19.89	18.48	1
		$V_S - T_{18}$	39.79	8.22	12.43	18.084	1
20/9	1.5	$F_{0A} - T_9$	121.26	6.96	37.89	15.312	1
		$V_S - T_{29}$	475.09	2.16	49.49	14.256	3

Figure 4.16 shows the closed loop responses of the control structure to +%20 step change in the production rate handle, F_{0B} . The column shuts down in the face of this disturbance for all three cases.

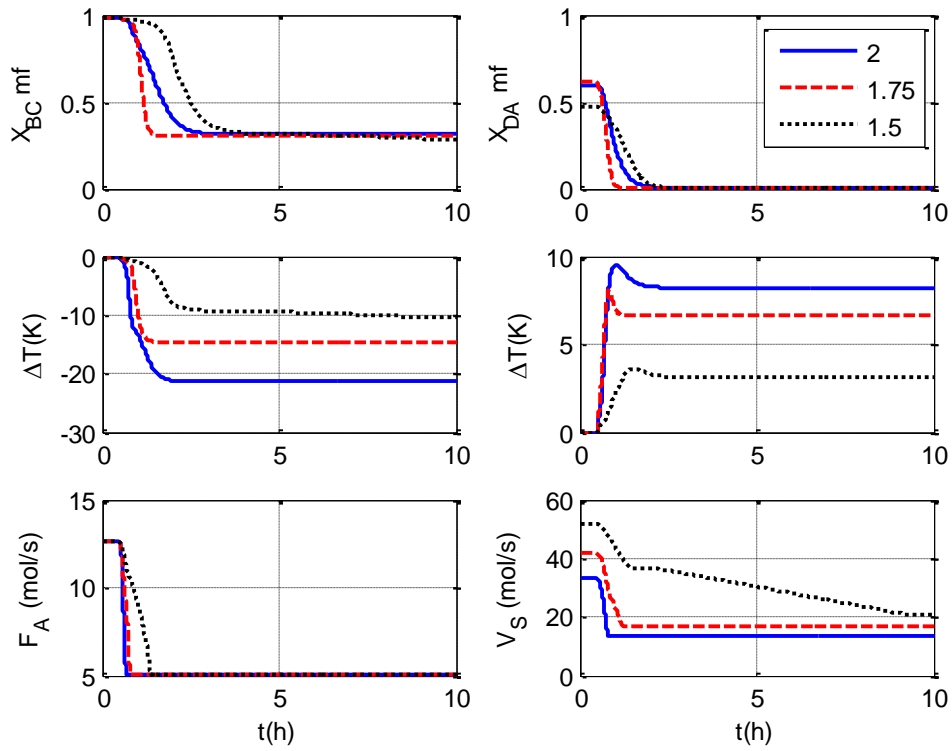


Figure 4.16: Result of Control Structure CS1: +20% F_{0B} Step Change

4.4.2. Control Structure CS2

Figure 4.17 gives the results of the sensitivity and SVD analysis for CS2 where F_{0B} and V_S are the manipulated variables. According to the results, the top of the reactive section is the most sensitive region for both manipulated variables. These results are also supported by the SVD analysis results. The results show that the sensitivity of trays for F_{0B} and V_S increases when relative volatility changes from 2 to 1.75, and decreases when it is decreased to 1.5. The control loops and PI controller parameters are given in Table 4.7 for each case.

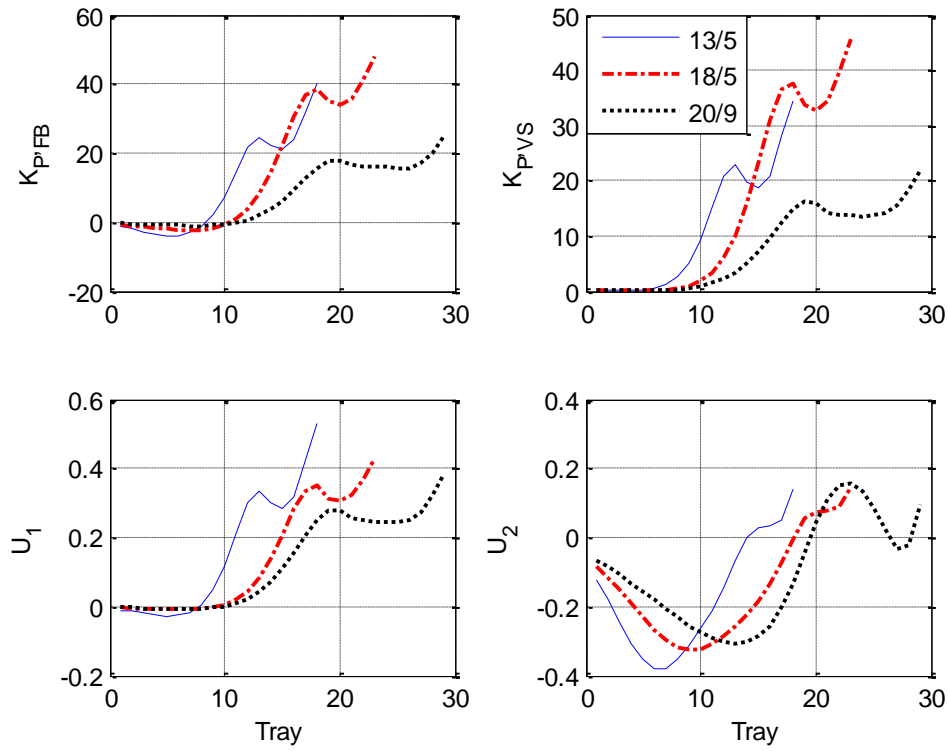


Figure 4.17 : Steady-State Gains and SVD Analysis

Table 4.7. Tuning Parameters of CS2

Design	α_{390}	Control Loop	K_U	P_U (min)	K_C	τ_I (min)	f
13/5	2	$V_S - T_{17}$	23.58	15.48	7.37	34.06	1
		$F_{0B} - T_{18}$	125.07	3.42	39.09	7.54	1
18/5	1.75	$V_S - T_{22}$	7.76	4.8	2.48	10.56	1
		$F_{0B} - T_{23}$	72.09	5.1	22.53	11.22	1
20/9	1.5	$V_S - T_{28}$	13.75	85.5	4.3	188.1	1
		$F_{0B} - T_{29}$	979.2	3.06	106.02	20.19	3

Figure 4.18 shows the closed loop responses of the control structure to $\pm 20\%$ step change in the production rate handle, F_{0A} . The systems are dynamically stable and both controlled temperatures turn back to their set points. However, the purity of the bottoms product settles down to a new steady state instead of turning back to its desired specification.

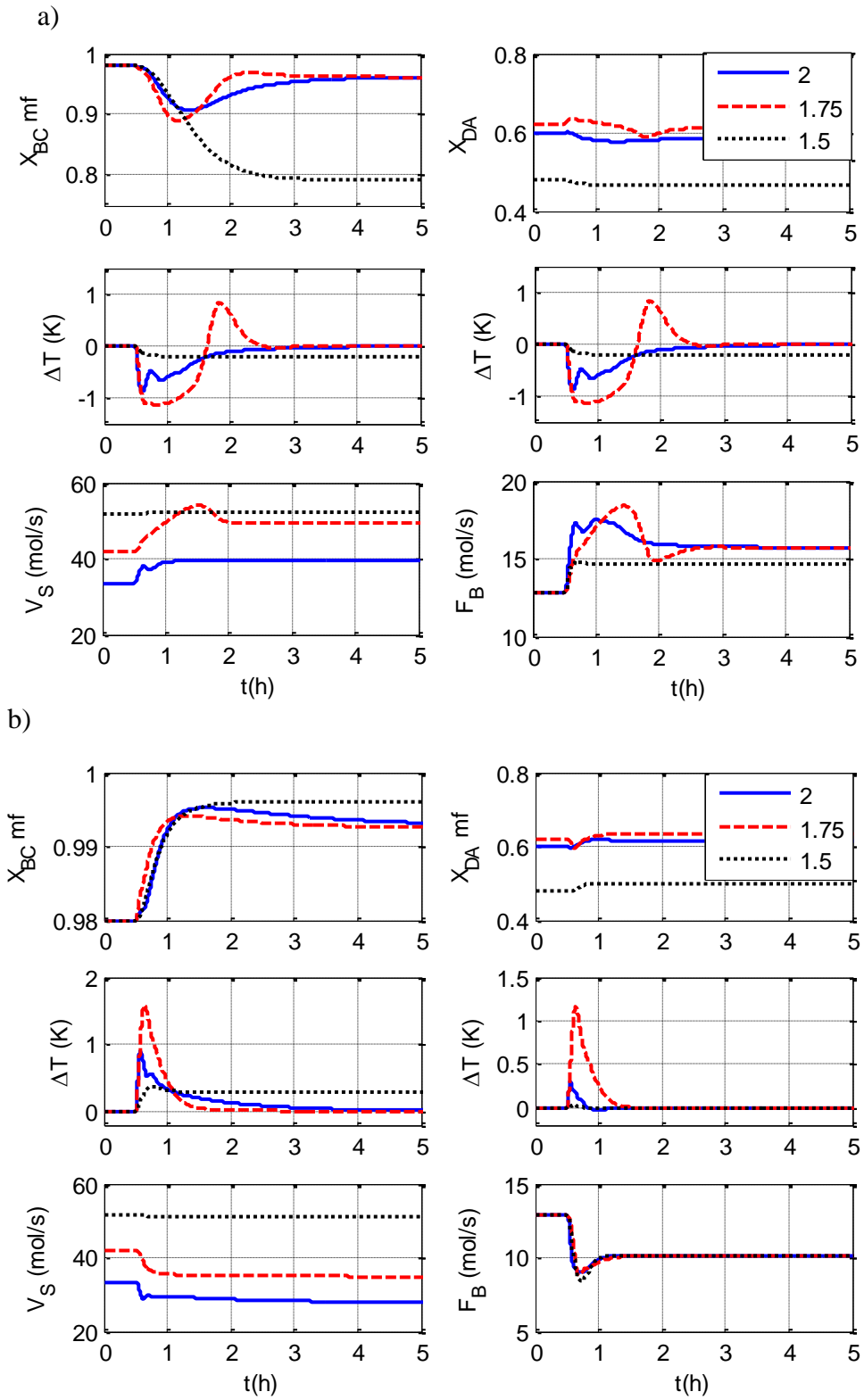


Figure 4.18: Result of Control Structure CS2: a) +20% F_{0A} b) -20% F_{0A}

4.4.3. Control Structure CS3

Figure 4.19 shows the results of the steady-state gains and SVD analysis for CS3. The manipulated variables for this control structure are F_{0A} and F_{0B} . The results indicate that the most sensitive trays for the fresh feed flow rates F_{0A} and F_{0B} are in the stripping section and at the top of the reactive zone, respectively. As the relative volatilities decrease, the sensitivity of trays for F_{0A} gets smaller. For each relative volatility case, the controller loops and PI controller parameters are given in Table 4.8.

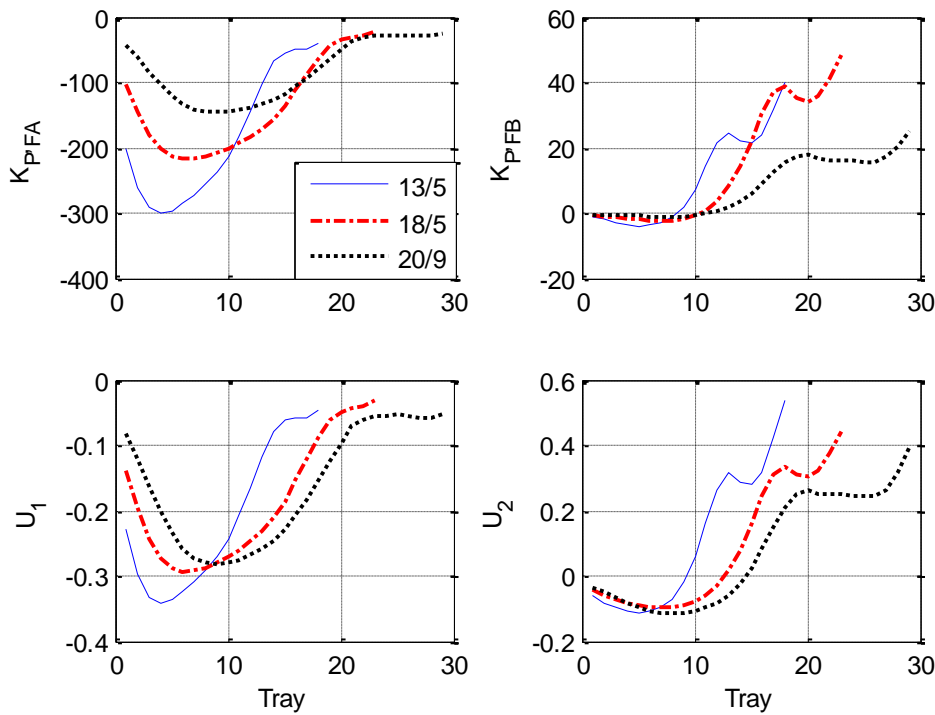
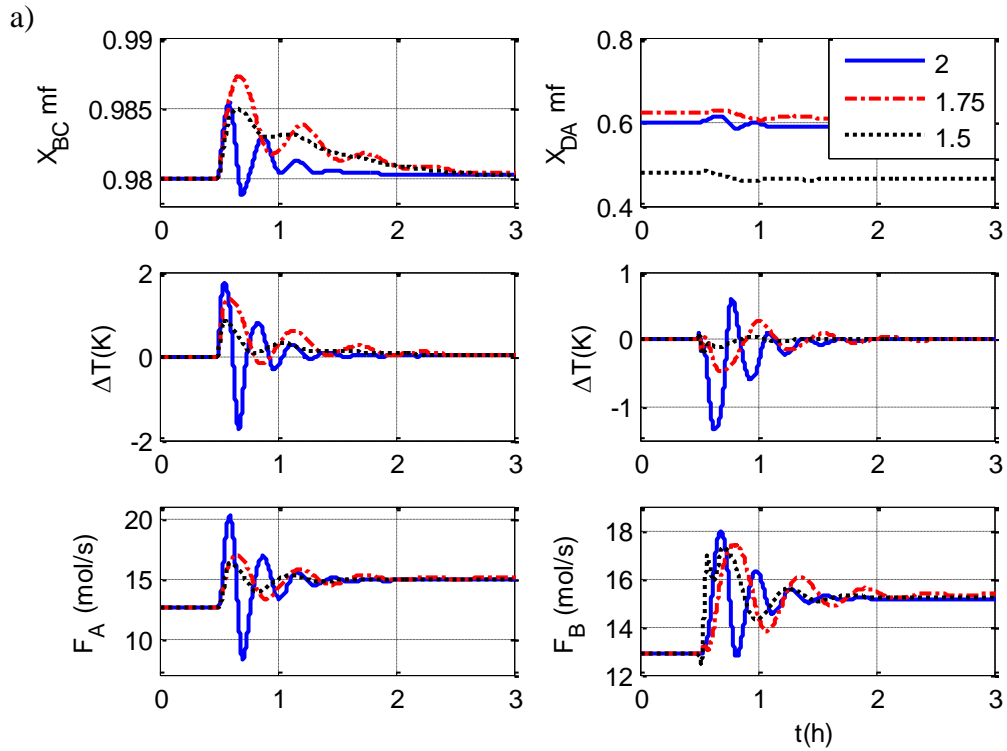


Figure 4.19: Steady-State Gains and SVD Analysis

Table 4.8 : Tuning Parameters

Design	α_{390}	Control Loop	K_U	P_U (min)	K_C	τ_I (min)	F
13/5	2	$F_{0A} - T_4$	53.05	7.62	16.58	16.764	1
		$F_{0B} - T_{18}$	125.07	3.42	13.03	22.572	3
18/5	1.75	$F_{0A} - T_6$	72.92	35.76	22.79	19.16	1
		$F_{0B} - T_{23}$	72.09	5.1	22.53	11.22	1
20/9	1.5	$F_{0A} - T_9$	113.48	9.12	35.46	20.06	1
		$F_{0B} - T_{29}$	979.2	3.06	106.02	20.19	3

Figure 4.20 and Figure 4.21 give the closed loop responses of control structure CS3 for the optimum designs. In Figure 4.20A, the disturbance is a positive 20% step change in the production rate handle V_S . Figure 4.20B gives results for a negative 20% step change in V_S . On the other hand, Figure 4.21A shows the closed loop response when the composition z_{0A} of the fresh feed F_{0A} is changed from pure A ($z_{0A(A)} = 1$) to a mixture of A and B ($z_{0A(A)} = 0.95$ and $z_{0A(B)} = 0.05$). Figure 4.21B gives the closed loop response of the case where the composition z_{0A} of the fresh feed F_{0A} is changed from pure A ($z_{0A(A)} = 1$) to a mixture of A and C ($z_{0A(A)} = 0.95$ and $z_{0A(C)} = 0.05$). It is observed that the systems are dynamically stable for a wide range of disturbances. The column settles down to its steady state operating conditions within 3 h.



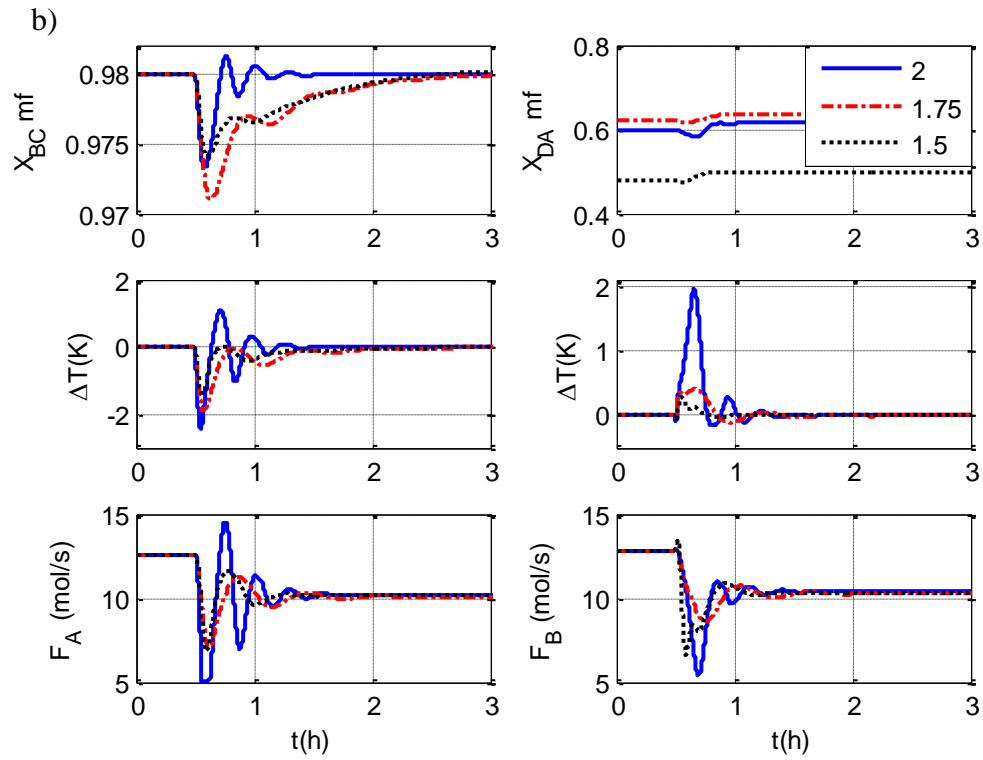
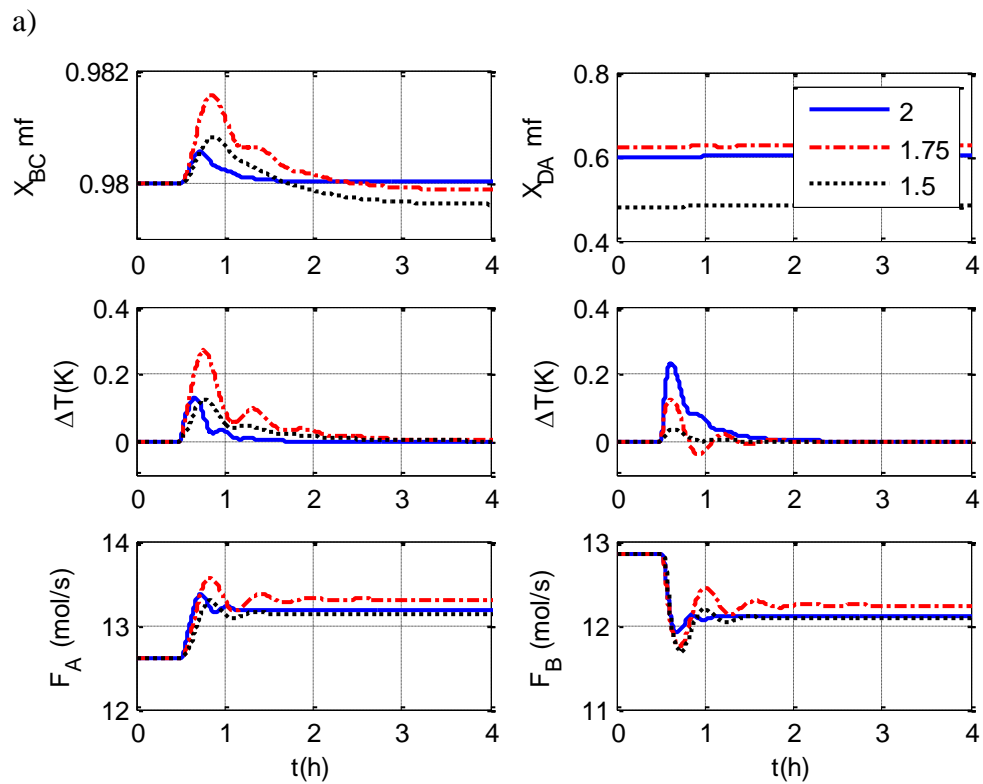


Figure 4.20 : Result of Control Structure CS3: a) +20% VS b) -20% VS



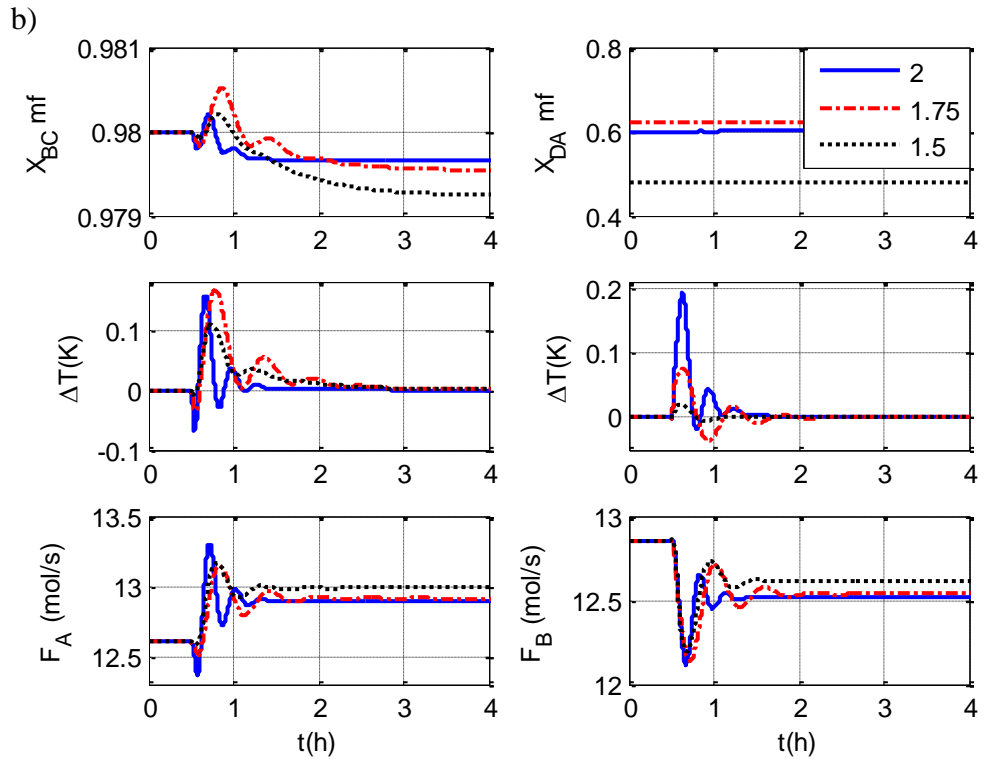


Figure 4.21 : Result of Control Structure CS3: a) $z_{0A(B)} = 0.05$, and b) $z_{0A(C)} = 0.05$

5. CONCLUSION

In this study, the effects of relative volatility of components on steady state design and temperature based inferential control of an ideal ternary system with two reactants and one product have been examined.

Firstly, a steady state column design has been built for the chemicals, which are assumed having relative volatilities between the adjacent components constant at 2. The RD column has been optimized using three optimization variables such as the number of stripping section, number of reactive section and operating pressure. The objective of the optimization problem was to minimize the Total Annual Cost (TAC).

Then, chemicals having temperature-dependent volatilities are fed to the existing column. It has been found that the system needs more vapor boilup as the relative volatilities get closer, which results in an increase of the energy cost. The increase of vapor boilup also affects column diameter and heat transfer areas of reboiler and condenser. Therefore, the increase in the capital and energy costs results in an increase of the total annual cost as the relative volatilities get closer.

Next, optimum steady state designs have been obtained for the chemicals having temperature-dependent relative volatilities. In this case, besides the increasing values of vapor boilups, column diameter and the heat transfer areas of reboiler and condenser, RD column requires more separation trays as relative volatilities get closer.

In the control part of the study, three different temperature based inferential control structures have been investigated. Sensitivity analysis and Singular Value Decomposition (SVD) method have been used to choose the most sensitive tray in the columns for the change of manipulated variable in designed control structures. Temperature loops have been adjusted by the Relay Feedback Test (ATV) method. Then, the performance of control structures has been examined in the face of different disturbances. The results show that control structure CS3, where the fresh feed streams are manipulated to control the tray temperatures, has been successful in

handling the disturbances for RD columns including ternary systems. On the other hand, no significant effect of the relative volatilities has been observed on the temperature based inferential control of the ternary RD columns.

REFERENCES

- [1] **Yu, C.C., Luyben, W.L.** 2008: Reactive Distillation Design And Control, John Wiley & Sons, Inc
- [2] **Sundmacher, K, Kienle, A.,** 2003: Reactive Distillation: Status and Future Directions. Weinheim, Germany
- [3] **Taylor, R., Krishna, R.,** 2000: Modeling Reactive Distillation, Chem Eng Sci, Vol. 55, pp. 5183–5229.
- [4] **Backhaus, A.A.,** 1921: Continuous Processes for The Manufacture of Esters, U.S. Patent 1,400,849.
- [5] **Kister, H. J.,** 1992: Distillation Design, McGraw-Hill Inc., New York
- [6] **Holland, CD.,** 1981: Fundamentals of Multicomponent Distillation, New York, McGraw-Hill
- [7] **Suzuki, I., Yagi, H., Komatsu, H. and Hirata, M** 1971: Calculation of Multicomponent Distillation Accompanied by Chemical Reaction. J. Chem. Eng., Japan, 4, 26-33.
- [8] **Aljeski, K., Duprat, F.,** 1996: Dynamic Simulation of the Multicomponent Reactive Distillation Chem. Eng. Sci., 51, 4237-4252.
- [9] **Sneesby, M. G., Tade, M. O., Datta, R. and Smith, T. N.,** 1997: ETBE Synthesis via Reactive Distillation. 1. Steady-State Simulation and Design Aspects. Ind. Eng. Chem. Res., 36, 1855-1869.
- [10] **Kumar, A., Daoutidis, P.,** 1999: Modeling, Analysis, Analysis and Control of Ethylene Glycol Reactive Distillation Column, AIChE J. 45, 51–68.
- [11] **Krishnamurthy, R. and Taylor, R.,** 1985: A Nonequilibrium Stage Model of Multicomponent Separation Processes. AIChE J., 32, 449-465.
- [12] **Higler, A., Taylor, R., & Krishna, R.,** 1998:. Modeling of a Reactive Separation Process Using a Nonequilibrium Stage Model, Computers & Chemical Engineering, 22, pp. 111- 118.
- [13] **Lee, J.H., Dudukovic, M.P.,** 1998: A Comparison of the Equilibrium and Nonequilibrium Models for a Multicomponent Reactive Distillation Column, Comput. Chem. Eng. 23, 159–172.
- [14] **Baur, R., Higler, A., Taylor, R., & Krishna, R.,** 2000: Comparison of Equilibrium Stage and Nonequilibrium Stage Models for Reactive Distillation, Chemical Engineering Journal 76, 33–47
- [15] **Kaymak D.B., Luyben W.L.,** 2004: A Quantitative Comparison of Reactive Distillation with Conventional Multi-Unit Reactor/Column/Recycle

Systems for Different Chemical Equilibrium Constants, Ind Eng Chem Res., 43, 2493–2507.

- [16] **Kaymak DB, Luyben WL**, 2004: Effect of the Chemical Equilibrium Constant on the Design of Reactive Distillation Columns, Ind Eng Chem Res., 43, 3666-3671
- [17] **Luyben, W. L., Pszalgowski, M. K., Schaefer, M. R. and Siddons, C.**, 2004: Design and Control of Conventional and Reactive Distillation Processes for the Production of Butyl Acetate, Ind. Eng. Chem. Res., 43, pp. 8014-8025
- [18] **Kaymak D.B., Luyben W.L., Smith IV O.J.**, 2004: Effect of Relative Volatility on the Quantitative Comparison of Reactive Distillation and Conventional Multi-Unit Systems. Ind Eng Chem Res., 43:3151–3162.
- [19] **Tung S.T., Yu C.C.**, 2007: Effects of Relative Volatility Ranking to the Design of Reactive Distillation, AIChE J., 53, 1278-1297
- [20] **Luyben W.L.**, 2007: Effect of Kinetic and Design Parameters on Ternary Reactive Distillation Columns, Ind. Eng. Chem. Res. 46, 6944-6952
- [21] **Hauan, S., Hertzberg, T., & Lien, K. M.**, 1997: Multiplicity in Reactive Distillation of MTBE, Computers and Chemical Engineering, 21, 1117-1124.
- [22] **Nijhuis, S.A., Kerkhof, F.J.P.M. and Mak, A.N.S.**, 1993: Multiple Steady State During the Reactive Distillation of Methyl Tert-Butyl Ether, Ind Eng Chem Res, 32(11), 2767–2774.
- [23] **Ciric, A. R.; Miao, P.**, 1994: Steady-State Multiplicities in an Ethylene Glycol Reactive Distillation Column, Ind. Eng. Chem. Res., 33, 2738-2748.
- [24] **Sneesby, M. G.; Tade, M. O.; Smith, T. N.**, 1998: Steady-State Transitions in the Reactive Distillation of MTBE. Comput. Chem. Eng., 22, 879.
- [25] **Singh, B. P., Singh, R., Pavan Kumar, M. V.; Kaistha, N.**, 2005: Steady State Analysis of Reactive Distillation using Homotopy Continuation, Chem. Eng. Res. And Des., 83, 959-968
- [26] **Roat, S., Downs, J. J., Vogel, E. F. and Doss, J. E.**, 1986: Integration of Rigorous Dynamic Modeling and Control System Synthesis for Distillation Columns, Chem. Pro. Control, pp. 99-138
- [27] **Bock, H., Wozny, G., & Gutsche, B.**, 1997: Design and Control of a Reaction Distillation Column Including The Recovery System, Chem. Eng. and Processing., 36, 101-109.
- [28] **Kumar, A., and P. Daoutidis**, 1999: Modeling, Analysis and Control of Ethylene Glycol Reactive Distillation Column, AIChE Journal, 45, 51
- [29] **Sneesby, M. G., Tade, M. O., Smith, D. R., and T. N.**, 1999: Two Point Control of Reactive Distillation Column for Composition and Conversion, J. Pro. Control, Vol. 9, pp. 19-31,
- [30] **Al-Arfaj, M. A., Luyben, W. L.**, 2000: Comparison of Alternative Control Structures for an Ideal Two-Product Reactive Distillation Column, Ind. Eng. Chem. Res., vol. 39, pp. 3298-3307

- [31] **Estrada-Villagrana, A., Bogle, I., Fraga, E. and Gani, R.,** 2000: Analysis of Input-Output Controllability In Reactive Distillation Using The Element Model, European Symposium on Computer Aided Process Engineering, 10, 157-162.
- [32] **Vora, N., and Daoutidis, P.,** 2001: Dynamics and Control of an Ethyl Acetate Reactive Distillation Column, Ind. Eng. Chem. Res, vol. 40, pp. 833-849
- [33] **Al-Arfaj, M. A., Luyben, W. L.,** 2002, Comparative Control Study of Ideal and Methyl Acetate Reactive Distillation, Chem. Eng. Sci., vol. 24, pp. 5039-5050
- [34] **Al-Arfaj, M. A., Luyben, W. L.,** 2002, Control Study of Ethyl Tert-Butyl Ether Reactive Distillation, Ind. Eng. Chem. Res., vol. 41, pp. 3784-3796
- [35] **Al-Arfaj, M. A., Luyben, W. L.,** 2002, Control of Ethylene Glycol Reactive Distillation Column, AIChE J., vol. 48, pp. 905
- [36] **Wang, S., Wong, D. S. H., Lee, E.,** 2003: Effect of Interaction Multiplicity on Control System Design for a MTBE Reactive Distillation Column, J. Pro. Control, Vol. 13, pp. 503-515
- [37] **Kaymak, D.B. and Luyben, W.L.,** 2006: Evaluation of a two-temperature control structure for a two-reactant/two-product type of reactive distillation column, Chem. Eng. Sci. 61, 4432-4450
- [38] **Kaymak, D.B. and Luyben, W.L.,** 2005: Comparison of Two Types of Two-Temperature Control Structures for Reactive Distillation Columns, Ind Eng Chem Res, 44(13), 4625–4640.
- [39] **Kumar, M.V.P., Kaistha, N.,** 2007: Temperature Based Inferential Control of a Methyl Acetate Reactive Distillation Column, Trans. Inst. Chem. Eng., Part A, 85, 1268-1280.
- [40] **Luyben, W.L.,** 2007: Control of Ternary Reactive Distillation Columns with and without Chemically Inert Components, Ind. Eng. Chem. Res., 46, 5576-5590
- [41] **Kumar, M.V.P., Kaistha, N.,** 2008: Steady-State Multiplicity and Its Implications on the Control of an Ideal Reactive Distillation Column, Ind. Eng. Chem. Res., 47, 2778-2787
- [42] **Kumar, M.V.P., Kaistha, N.,** 2008: Role of Multiplicity In Reactive Distillation Control System Design, Journal of Process Control 18, 692-706
- [43] **Kumar, M.V.P., Kaistha, N.,** 2008: Decentralized Control of a Kinetically Controlled Ideal Reactive Distillation Column, Chem. Eng. Sci. 63, 228-243
- [44] **Kumar, M.V.P., Kaistha, N.,** 2009: Reactive Distillation Column Design for Controllability: A Case Study” Chem. Eng. Res. & Des. 48, 606-616
- [45] **Kumar, M.V.P., Kaistha, N.,** 2009: Evaluation of Ratio Control Schemes in a Two-Temperature Control Structure for a Methyl Acetate Reactive Distillation Column” Chem. Eng. Res. & Des. 87, 216-225

- [46] **Jelink, J., & Halvacek, V.**, 1976: Steady State Countercurrent Equilibrium Stage Separation with Chemical Reaction by Relaxation Method, Chem. Eng. Comm., 79–85.
- [47] **Komatsu, H.**, 1977: Application of The Relaxation Method for Solving Reacting Distillation Problems, Journal of Chemical Engineering of Japan, 10, p. 200-2006.
- [48] **Marlin, E.T.**, 2000: Designing Processes and Control Systems for Dynamic Performance, McGraw-Hill, Singapore
- [49] **Michael, W.L., Luyben, W.L.**, 1997: Essentials of Process Control, The McGraw-Hill, Singapore
- [50] **Moore, C.F.**, 1992: Selection of Controlled and Manipulated Variables, in Luyben, W.L. (ed.). Practical Distillation Control, Van Nostrand Reinhold, New York, USA
- [51] **Ohio State Web Site**, <http://www.ling.ohio-state.edu/~kbaker/pubs/Singular_Value_Decomposition_Tutorial.pdf> accessed at 25.04.2010.
- [52] **Luyben, W.L.**, 2006: Evaluation of Criteria for Selecting Temperature Control Trays in Distillation Columns”, Journal of Process Control 16, 115–134
- [53] **Kaymak, D.B., Sunar, G.**, 2009: Effect of Feed Tray Location on Temperature-Based Inferential Control of Double Feed Reactive Distillation Columns, Ind. Eng. Chem. Res., 48, 11071–11080
- [54] **Aström, K. J.; Hagglund, T.**, 1984: Automatic Tuning of Simple Regulators with Specifications on Phase and Amplitude Margins. Automatica, 20, 645.
- [55] **Shen, S. H., Yu, C. C.**, 1994: Use of Relay-Feedback Test for Automatic Tuning of Multivariable Systems. AIChE J., 40, 627.
- [56] **Luyben, W. L.**, 2001: Getting More Information from Relay Feedback Tests. Ind. Eng. Chem. Res., 40 (20), 4391.
- [57] **Thyagarajan, T.**, 2003: Yu, C. C. Improved Auto-tuning Using Shape Factor from Relay Feedback. Ind. Eng. Chem. Res., 42, 4425.
- [58] **Tyreus, B. D.; Luyben, W. L.**, 1992: Tuning PI Controllers for Integrator-Deadtime Processes. Ind. Eng. Chem. Res., 31, 2625.

CURRICULUM VITA



Candidate's full name: Denizhan Yılmaz

Place and date of birth: İstanbul, 01.01.1983

Permanent Address: Abbasağa Mah. Ortaoyuncu Sk. Babaevi Apt. No 1 D.1
Beşiktaş İstanbul

Universities and Colleges attended:

B. Sc. : Yıldız Technical University, Chemistry, (2001 – 2006)

M.Sc.: İstanbul Technical University, Chemical Engineering, (2008-2010)

Publications:

- Yılmaz D., Kaymak D. B., 2010: Controllability of the Optimum Design for a Ternary Reactive Distillation Column. *6th Chemical Engineering Conference for Collaborative Research in Eastern Mediterranean Countries*, March 7-12, 2010 Antalya, Turkey.